Available online at www.sciencedirect.com
SCIENCE DIRECT
Virology 348 (2006) 309–327
VIROLOGY
www.elsevier.com/locate/yviro

Characterization of Kaposi's sarcoma-associated herpesvirus (KSHV) K1 promoter activation by Rta

Brian S. Bowser [a], Stephanie Morris [b], Moon Jung Song [c,1], Ren Sun [c], Blossom Damania [a,*]

[a] Department of Microbiology and Immunology and Lineberger Comprehensive Cancer Center, CB #7295 University of North Carolina, Chapel Hill, NC 27599, USA
[b] Department of Biochemistry and Biophysics, University of North Carolina at Chapel Hill, Chapel Hill, NC 27599, USA
[c] Department of Molecular and Medical Pharmacology, the UCLA AIDS Institute, the Jonnson Comprehensive Cancer Center, and the Molecular Biology Institute, University of California at Los Angeles, Los Angeles, CA 90095, USA

Received 18 July 2005; returned author for revision 7 December 2005; accepted 8 February 2006
Available online 20 March 2006

Abstract

The *K1* gene of Kaposi's sarcoma-associated herpesvirus (KSHV) encodes a 46-kDa transmembrane glycoprotein that possesses transforming properties, initiates signaling pathways in B cells, and prevents apoptosis. Here, we demonstrate a mechanism for activation of the K1 promoter by the Rta transactivator. Electrophoretic mobility shift assay (EMSA) analysis of the K1 promoter demonstrated that purified Rta protein bound to the K1 promoter at three locations, independent of other DNA-binding factors. Transcriptional assays revealed that only two of these Rta DNA-binding sites are functionally significant, and that they could impart Rta responsiveness to a heterologous E4 TATA box promoter. In addition, TATA-binding protein (TBP) bound to a TATA box element located 25 bp upstream of the K1 transcription start site and was also shown to associate with Rta by coimmunoprecipitation analysis. Rta transactivation may therefore be mediated in part through recruitment of TBP to target promoters.

Keywords: KSHV; HHV8; K1; Rta; Orf50; Transcription

Introduction

Kaposi's sarcoma-associated herpesvirus (KSHV), also known as human herpesvirus 8 (HHV8), has been linked to the development of Kaposi's sarcoma (KS) and is also associated with two B cell lymphomas—primary effusion lymphoma (PEL) and multicentric Castleman's disease (MCD) (Cesarman et al., 1995; Ganem, 1998; Moore and Chang, 1995; Soulier et al., 1995). KSHV is closely related to rhesus monkey rhadinovirus (RRV), murine herpesvirus 68, and herpesvirus saimiri (HVS) and based on sequence homology has been classified as a gamma 2 herpesvirus or rhadinovirus (Albrecht et al., 1992; Alexander et al., 2000; Virgin et al., 1997).

The first open reading frame of KSHV, OrfK1, encodes a 46-kDa transmembrane glycoprotein(Lee et al., 1998b). K1 is located at the far left end of the KSHV genome, a position occupied by the saimiri transformation-associated protein (STP) in the HVS genome and R1 in the RRV genome (Damania et al., 1999; Murthy et al., 1989). Although K1 and R1 occupy positions equivalent to HVS STP, they possess no obvious sequence similarity with STP (Damania et al., 1999; Lee et al., 1998b; Murthy et al., 1989). HVS STP is necessary for the immortalization of primary T lymphocytes and the development of lymphomas in marmosets(Duboise et al., 1998). Like its positional homolog, K1 has also been shown to immortalize marmoset lymphocytes to IL-2-independent proliferation when substituted for STP in the context of HVS. K1 induces foci formation and morphological changes in Rat-1 fibroblasts (Lee et al., 1998b). Finally, transgenic animals expressing K1 develop spindle-cell sarcomatoid tumors and malignant plasmablastic lymphomas (Prakash et al., 2002). K1 is expressed in KS lesions, primary effusion

* Corresponding author. Mailing Address: Lineberger Comprehensive Cancer Center, CB #7295 University of North Carolina, Chapel Hill, NC 27599, USA. Fax: +1 919 966 9673.
E-mail address: damania@med.unc.edu (B. Damania).
[1] Present address: Division of Biotechnology, College of Life Sciences and Biotechnology, Korea University, Seoul 136-713, Republic of Korea.

0042-6822/$ - see front matter © 2006 Elsevier Inc. All rights reserved.
doi:10.1016/j.virol.2006.02.007

lymphoma cell lines, and multicentric Castleman's disease tissues (Bowser et al., 2002; Lagunoff and Ganem, 1997; Lee et al., 2003; Samaniego et al., 2001). We have previously demonstrated that the K1 promoter is activated by expression of Rta in B cells, endothelial and epithelial cells (Bowser et al., 2002). The K1 protein contains an immunoreceptor tyrosine-based activation motif (ITAM) in its cytoplasmic tail(Lee et al., 1998a). Expression of K1 protein in B cells leads to the phosphorylation of signaling proteins, mobilization of intracellular calcium, and ultimately the activation of transcription factors such as NFAT and AP-1(Lee et al., 2002; Samaniego et al., 2001). Signaling through the ITAM has also been shown to activate the Akt signaling pathway and to inhibit apoptosis induced by FKHR proteins and Fas signaling (Tomlinson and Damania, 2004). Samaniego et al. demonstrated that K1 expression leads to the activation of NF-κB-dependent promoters(Samaniego et al., 2001).

Similar to other gammaherpesviruses, KSHV establishes a latent infection in the majority of infected cells. During latency, only a small subset of genes is expressed to prevent cell death and maintain the viral genome in a circular, episomal state. However, in a small subset of cells within KS lesions and in cultured PEL cells, the virus is reactivated and expresses lytic genes that ultimately lead to the production of progeny virions (Renne et al., 1996; Staskus et al., 1997, 1999; Zhong et al., 1996). This limited lytic reactivation is apparently vital to the maintenance of KS lesions since treatment with ganciclovir was shown to reduce the risk of KS development(Martin et al., 1999).

The switch from latent to lytic KSHV infection is initiated by the product of open reading frame 50 (Orf50), also known as replication and transcription activator (Rta), ART, or Lyta (Gradoville et al., 2000; Lukac et al., 1998, 1999; Sun et al., 1998). Rta possesses an amino-terminal DNA-binding domain, a dimerization domain, a serine threonine-rich tract, two nuclear localization signals (NLS), and a carboxy-terminal activation domain. This protein architecture is reminiscent of other transcription factors. KSHV Rta is functionally homologous to the BRLF1 gene product encoded by Epstein–Barr virus (EBV) and the Orf50 proteins encoded by rhesus rhadinovirus (RRV), murine gammaherpesvirus 68 (MHV68), and herpesvirus saimiri (HVS) (DeWire et al., 2002; Liu et al., 2000; Sun et al., 1998; Wu et al., 2000). A comparison of KSHV, RRV, and MHV68 Rta proteins demonstrated that all three proteins are capable of activating transcription from several KSHV promoters, indicating that the Rta proteins are closely related (Damania et al., 2004). Additionally, HVS Orf50 has also been shown to reactivate the HVS lytic cycle and to function as a transcriptional activator of delayed early promoters (Goodwin et al., 2001; Walters et al., 2004; Whitehouse et al., 1997). For KSHV, the Rta protein alone is both necessary and sufficient to induce lytic reactivation (Gradoville et al., 2000; Sun et al., 1998). KSHV Rta transcripts are detected within 1 h after TPA treatment (Lukac et al., 1999). Expression of Rta leads to the activation of downstream lytic genes and ultimately the production of progeny virions (Gradoville et al., 2000; Lukac et al., 1999; Renne et al., 1996). However, expression of a dominant negative Rta mutant that lacks the carboxy terminal activation domain prevents spontaneous reactivation and induction by chemical inducers(Lukac et al., 1999). The various functions of the KSHV Rta protein have been well reviewed by West and Wood (2003).

Rta has been shown to transactivate the promoters of a number of lytic genes including K8 (K-bZIP), Orf57 (Mta), polyadenylated nuclear (PAN) RNA (nut-1), Kaposin (K12), K1, viral interleukin-6 (vIL-6), K5, K9, Orf59, thymidine kinase (TK), vGPCR, K14, Orf6, Orf9, and Orf50 (Bowser et al., 2002; Chen et al., 2000; Deng et al., 2002a, 2002b; Haque et al., 2000; Jeong et al., 2001; Liang et al., 2002; Lukac et al., 1998, 1999; Sakakibara et al., 2001; Song et al., 2001; Wang et al., 2001a; Zhang et al., 1998). This transactivation occurs through direct binding to Rta response elements (RRE) or through an association with other factors such as Oct-1, Sp1, RBP-Jκ (CSL), MGC2663, cAMP response element binding protein (CREB)-binding protein (CBP), c-Jun, and CCAAT/enhancer-binding protein-alpha (C/EBPα) (Gwack et al., 2001; Liang and Ganem, 2004; Liang et al., 2002; Sakakibara et al., 2001; Wang et al., 2001a, 2001b, 2003a, 2003b; Zhang et al., 1998).

For many of these promoters, transactivation occurs through direct binding to RREs in the promoter. Rta binds directly to the promoters of PAN, Kaposin, K8, Orf57, and vIL-6 (Chang et al., 2002; Deng et al., 2002b; Duan et al., 2001; Lukac et al., 1998, 1999; Song et al., 2002a, 2002b). Early analysis of Rta transactivation demonstrated that Rta bound to very similar response elements within the K8 and Orf57 promoters (Lukac et al., 2001). The Rta-binding sites within the PAN and Kaposin promoters are also very similar to each other (Chang et al., 2002), however, the K8, Orf57, and vIL-6-binding sites lack significant similarity to the PAN and Kaposin Rta-binding sites (Chang et al., 2002; Deng et al., 2002b; Duan et al., 2001; Lukac et al., 1998, 1999; Song et al., 2002a, 2002b). In an attempt to explain the apparent diversity associated with Rta binding, Liao et al. recently identified a pattern of A/T triplets that confer Rta responsiveness (Liao et al., 2003). A/T motifs separated by 7 or 17-bp GC-rich spacers were found in the K8, Orf57, PAN, and Kaposin promoters and may be responsible for mediating Rta binding to these promoters. However, the core Rta-binding site in the vIL-6 promoter does not appear to share this pattern (Deng et al., 2002b).

We have previously demonstrated that the K1 promoter is activated by expression of Rta in B cells, endothelial and epithelial cells (Bowser et al., 2002). The mechanism for this activation, however, was unknown. Here, we found that the activation of the K1 promoter by Rta occurs through direct DNA binding to three binding sites within the K1 promoter, independent of other DNA-binding proteins. Of these three sites, only two appear to be functionally significant, and either functional binding site is sufficient to provide Rta responsiveness to a heterologous promoter. Furthermore, two of the Rta-binding sites in the K1 promoter conform to the A/T nucleotide pattern described by Liao et al. (2003), but the third site represents a new Rta-binding sequence. We also demonstrate an

association of TBP with a TATA box located 25 bp upstream of the K1 transcription start site. Coimmunoprecipitation analysis revealed an association of Rta with TBP, suggesting that Rta may function in part to recruit TBP to the TATA box. Overall, our data suggest that Rta binds to the K1 promoter independent of other factors and may recruit TBP to promote K1 transcription.

Results

Identification of RTA responsive elements (RREs) in the K1 promoter

Our previous data demonstrated that the first 125 bp upstream of the K1 transcription start site are capable of functioning as a fully active promoter element (Bowser et al., 2002). To identify the sequences within this construct that contribute directly to K1 promoter activity, we constructed a panel of linker scanning mutants that contains sequential, 10-bp substitutions of the 125-bp K1 promoter element and 5′ untranslated region in the context of the pGL2-Basic luciferase vector (Promega). Overlapping *Bam*HI and *Nco*I restriction enzyme sites were substituted for the wild-type promoter sequence as shown in Fig. 1A. The integrity of the promoter mutants was confirmed by restriction digest (Fig. 1B) and sequencing. Each of the linker scanning mutant plasmids was cotransfected into KSHV-positive BCBL-1 B cells, KSHV-negative DG75 B cells, or HEK 293 cells with either a pcDNA3-Rta expression vector or empty pcDNA3 plasmid, and a β-galactosidase expression plasmid to control for transfection efficiency.

Although Rta could transactivate the wild-type −125K1p promoter 13.5-fold in BCBL-1 cells, several of the K1 promoter linker scanning mutants demonstrated a reduced responsiveness to Rta when compared to −125K1p. Linkers P8 (1.7-fold), P9 (3.0-fold), and P18 (2.4-fold) each displayed at least a 75% reduction in Rta responsiveness (shown by the dashed line) while linker P11 (5.1-fold) displayed more than a 50% reduction in Rta responsiveness (Fig. 2A). Luciferase reporter assays were also performed in DG75 B cells to corroborate the BCBL-1 data in an uninfected B cell line. In the context of DG75 B cells, the wild-type −125K1p was activated 17-fold. However, linker P11 (4.9-fold), linker P18 (7.3-fold), and linker P20 (7.0-fold) each demonstrated at least a 50% reduction in responsiveness to Rta compared with the wild-type K1 promoter (Fig. 2B). Rta responsiveness in uninfected HEK 293 cells closely resembled Rta responsiveness in DG75 cells (Supplementary Fig. 1). We hypothesized that since linkers P11 and P18 are less responsive to Rta in each cell line, they represent the most likely locations for Rta response elements.

The mutation introduced into K1 promoter linker scanning mutant P11 resulted in a decreased responsiveness to Rta, however, this mutation may have also affected the putative K1 TATA box which is located in the same region. An additional K1 promoter mutant was therefore generated in which mutations were introduced into sites predicted to disrupt the TATA box, while having a minimal effect on the responsiveness to Rta (TACTAATTTT to TGCGCATTTT). This mutant was transfected into BCBL-1 cells along with either a Rta expression vector or empty pcDNA3 vector, and promoter activity was assessed by luciferase assays. The activity of the K1 TATA mutant in the presence or absence of Rta was compared with the wild-type K1 promoter sequence. The K1 TATA mutation completely abolished basal promoter activity but retained 8.4-fold responsiveness to Rta (Fig. 2C). This is in contrast to the wild-type promoter element which possesses minimal basal activity in addition to being responsive to Rta. Collectively, these reporter assays demonstrate a partial uncoupling of the Rta response element and TATA box in the K1 promoter.

Rta binds the K1 promoter in an electrophoretic mobility shift assay (EMSA)

Our analysis indicates that Rta can activate the −125K1p promoter fragment. This activation may be mediated by a direct or indirect mechanism. Direct transactivation of the K1 promoter may occur through direct binding of Rta protein to response elements within the K1 promoter. Indirect mechanisms of K1 promoter activation include Rta binding to the K1 promoter by tethering to other bound transcription factors. Alternatively, it is possible that Rta expression activates other cellular or viral transcription factors, which in turn activate the K1 promoter. To determine whether Rta activates the K1 promoter through direct contact with Rta response elements, an electrophoretic mobility shift assay (EMSA) was performed with the entire 125-bp K1 promoter element. The Rta DNA-binding domain (amino acids 1–320) was expressed in BL21 (DE3)pLysS *Escherichia coli* (Stratagene) and purified by Ni-NTA agarose purification as described previously (Song et al., 2002b). This Rdbd protein was also tagged with a Flag epitope (Song et al., 2002b). Bacterially expressed Rta has previously been shown to bind Rta response elements in viral promoters by several laboratories (Liao et al., 2003; Lukac et al., 2001; Song et al., 2001, 2002b).

Rta has previously been shown to bind to a response element within the PAN promoter (Song et al., 2001). This response element was labeled and used in EMSA analysis to control for Rta binding. In Fig. 3A, the addition of purified Rdbd in lane 3 results in the formation of a shifted complex confirming the association of Rta with the PAN probe under these conditions. The mobility of this complex is further retarded by the addition of a monoclonal anti-FLAG antibody (lane 4), confirming that Rta is present in the shifted complex in lane 3. Together, these data indicate that the proper conditions were used to observe Rta binding. Fig. 3B shows the results of EMSA analysis of the 125-bp K1 promoter element with purified Rdbd. Lanes 1 and 2 represent probe alone and extract from untransformed BL21 cells, respectively. The addition of purified Rdbd in lane 3 results in the appearance of a complex with retarded mobility, suggesting that Rta can directly bind to the 125-bp K1 promoter fragment. To confirm that Rdbd is responsible for this shifted complex, monoclonal anti-FLAG antibody (Sigma) was

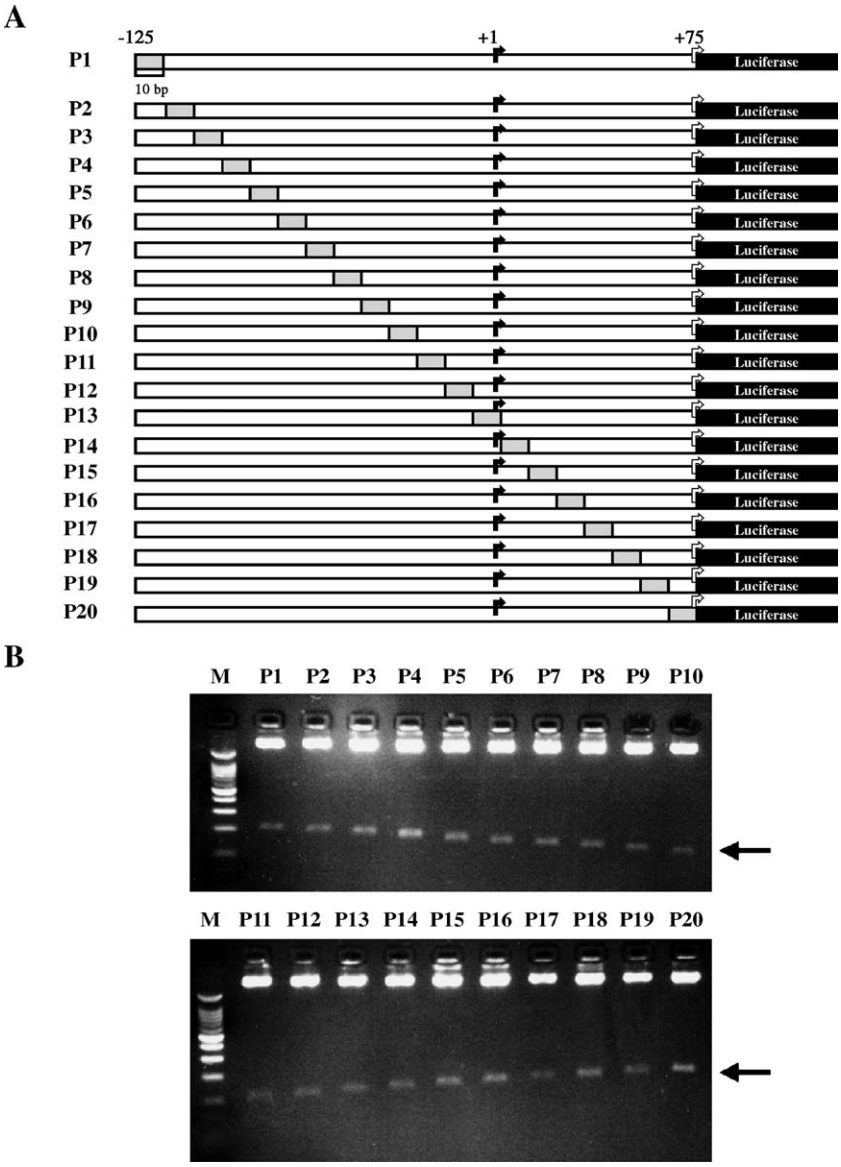

Fig. 1. Panel of K1 promoter linker scanning mutants. (A) Diagram of linker scanning mutant panel. Sequential, 10-bp substitutions were made to the K1 promoter element. Overlapping *Nco*I and *Bam*HI restriction enzyme sites were substituted for the wild-type promoter sequence. The gray boxes indicate the location of each mutation. Black arrows indicate the location of the transcription start site, while the white arrows indicate the translation start site. Base pair positions are given relative to the K1 transcription start site. The panel of K1 mutants was made in the context of the pGL2-Basic luciferase vector (Promega). (B) Confirmation of mutagenesis. Linker scanning mutants P1 through P10 were digested with *Nco*I and *Xho*I, while mutants P11 through P20 were digested with *Sac*I and *Nco*I to confirm mutagenesis. Digests were separated on a 1% agarose gel. Mutagenesis was also confirmed by plasmid sequencing (data not shown).

included in the binding reaction in lane 4. Anti-FLAG antibody further retarded the mobility of the shifted species present in lane 3, demonstrating that Rdbd is present in the shifted complex. These results indicate that purified Rdbd binds directly to the K1 promoter, independent of other DNA-binding proteins.

Identification of Rta-binding sites within the K1 promoter element

To identify the Rta-binding site(s) within the K1 promoter element, a panel of 30-bp K1 promoter probes was generated for use in additional EMSA experiments. Fig. 4 shows the alignment of these 30-mer probes with respect to the entire K1 promoter element. Probes A to D sequentially span the entire 125-bp K1 promoter element, while probes E to G overlap probes A/B, B/C, and C/D, respectively. Linker scanning mutant analysis indicated that the 5′ untranslated region sequence mutated in linker P18 is also important for Rta responsiveness (Figs. 2A and B). Therefore, probe H was designed to test a 30-bp fragment of the 5′ untranslated region immediately upstream of the translation start site.

EMSA analysis of the 30-bp probes was performed as before, but additional controls were added to further confirm the specificity of shifted and supershifted complexes. As a negative control, extracts were prepared from BL21 cells that were left

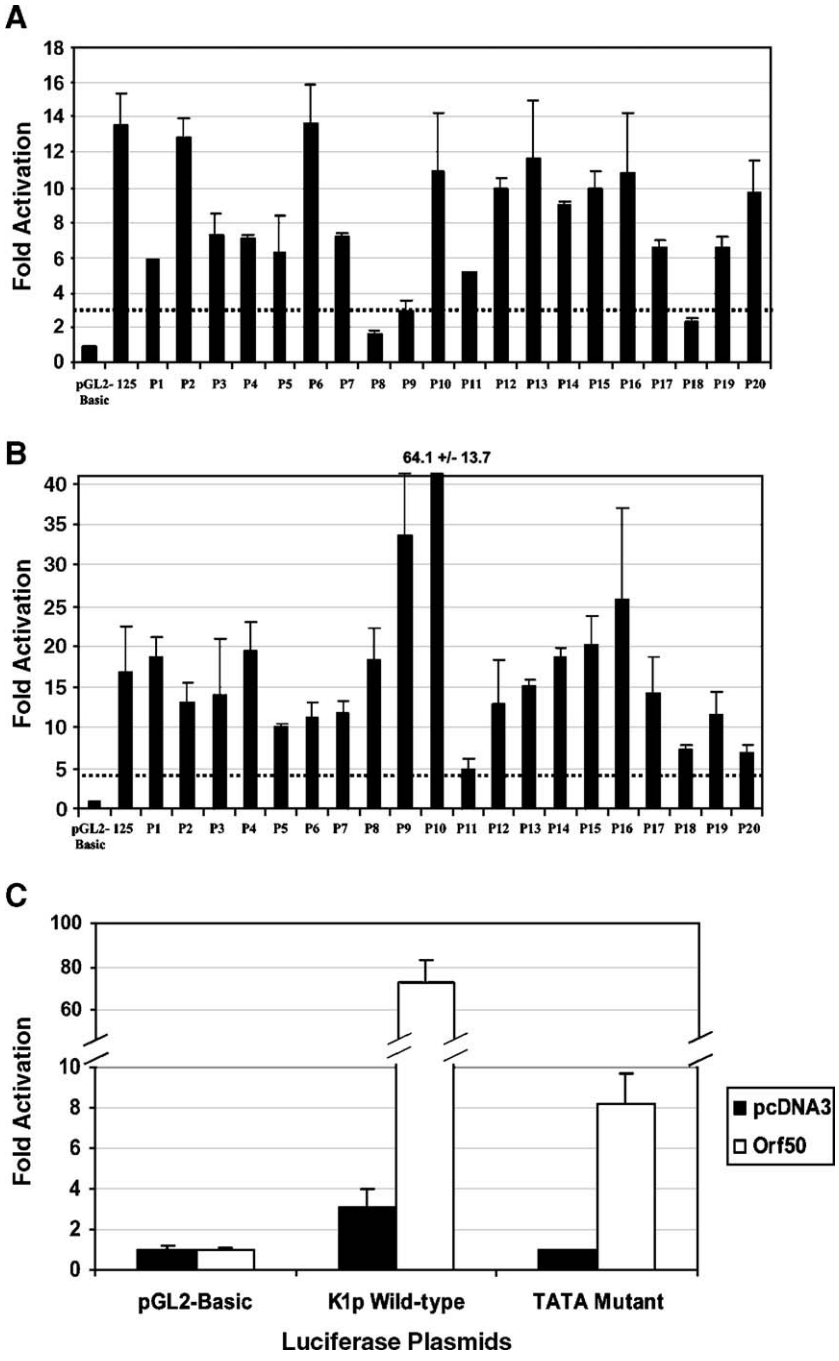

Fig. 2. Identification of Rta response element(s). Rta activation of K1 promoter linker scanning mutants in KSHV-positive BCBL-1 B cells (A) and KSHV-negative DG75 B cells (B). Each K1 promoter linker scanning mutant was cotransfected with a β-galactosidase expression vector to normalize for transfection efficiency, and either a pcDNA3-Rta expression vector or empty pcDNA3 plasmid. The activation of the promoter by Rta is represented as fold activation over pcDNA3-transfected controls. The dashed lines in panels A and B indicate a 75% reduction in responsiveness to Rta compared with the wild-type −125K1p plasmid. (C) Uncoupling of Rta transactivation and TATA box activity. A K1 promoter luciferase plasmid with a mutated TATA box (...TACTAATTTT... to ...TGCGCATTTT...) was cotransfected with a β-galactosidase expression vector to normalize for transfection efficiency, and either a pcDNA3-Rta expression vector or empty pcDNA3 plasmid. The activity of the mutant K1 promoter was compared with the activity of wild-type pGL2-Basic/-125K1p or empty pGL2-Basic. Promoter activity is represented as fold activation over empty pGL2-Basic luciferase vector.

untransformed but were subjected to the same IPTG induction and Ni-NTA purification as Rdbd-transformed cells. These negative control samples were used to demonstrate any background, nonspecific (NS) bands that may be carried through the Ni-NTA purification. In addition, competition experiments were performed in which an excess of unlabeled PAN Rta response element was added to the purified Rdbd protein prior to the addition of probe. The PAN Rta response element has previously been shown to bind very strongly to purified Rdbd (Song et al., 2002b).

EMSA analysis of each 30-mer K1 promoter probe demonstrated the presence of one or more nonspecific (NS)

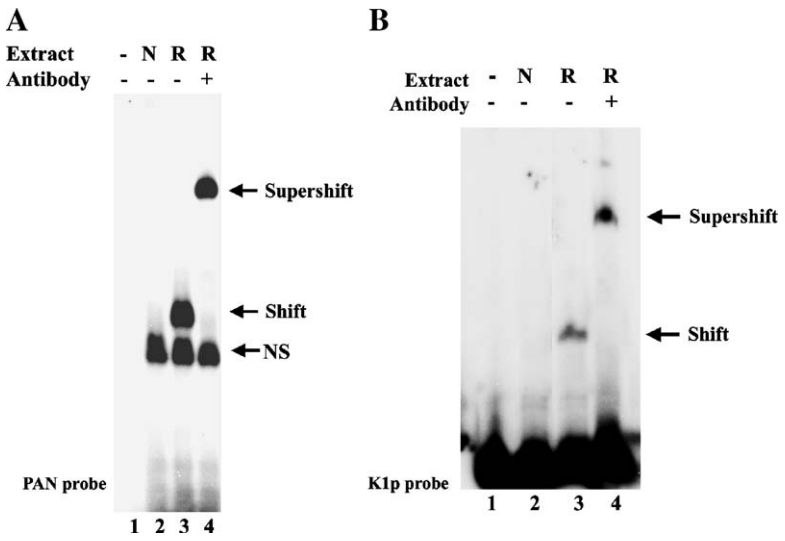

Fig. 3. Rta electrophoretic mobility shift assay of the K1 promoter. The Rta DNA-binding domain was expressed in BL21 *E. coli* and purified by Ni-NTA purification. The PAN Rta response element (A) or the K1 promoter (minus the 5′UTR) (B) was ^{32}P-labeled and used in a mobility shift assay with purified Rta DNA-binding domain. Lane 1: Probe alone, lane 2: untransformed BL21 negative control, lane 3: Rdbd shift, lane 4: Rdbd, anti-FLAG supershift.

background bands, contributed by the BL21 cells (Fig. 5). These background bands were present in extracts from both BL21 negative control extracts and purified Rdbd extracts. Monoclonal anti-FLAG antibody was unable to supershift these background bands regardless of which probe was being tested, indicating that these background bands are not the result of Rta binding and that the anti-FLAG antibody does not recognize and supershift these background bands.

Rdbd failed to bind to probes A, B, C, D, and F as shown in lane 4 of Figs. 5A, B, C, D, and F, respectively. However, probes E, G, and H each demonstrated specific shifts in the presence of Rdbd (Lane 4, Figs. 5E, G, H). These shifts were supershifted with the addition of anti-FLAG antibody, indicating that Rta is responsible for this shifted complex (Lane 5, Figs. 5E, G, H). Furthermore, incubation with an excess of unlabeled PAN RRE efficiently competes for Rdbd, thereby significantly reducing Rdbd-specific shifts and supershifts (lane 6, Figs. 5E, G, H), demonstrating that purified Rdbd specifically binds to probes E, G, and H in the K1 promoter.

Functional contribution of the three Rta-binding sites in the K1 promoter

EMSA analysis demonstrated the existence of three Rta-binding sites, two within the K1 promoter (E, G) and one within the 5′ untranslated region (H). Interestingly, two of these

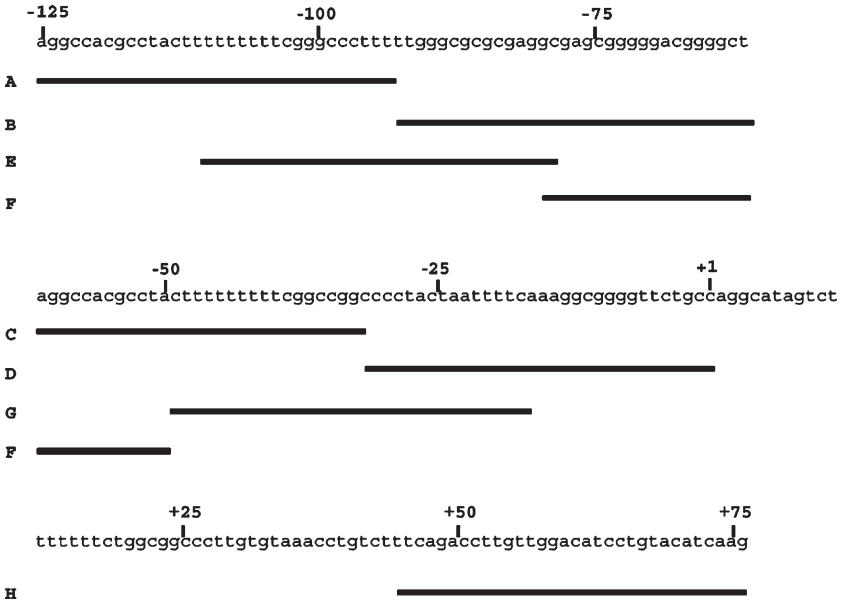

Fig. 4. Panel of K1 promoter EMSA probes. A panel of 30-mer K1 promoter probes was generated for use in Rta EMSA analysis. The full-length −125K1p promoter is indicated. The location of each probe is shown in comparison with the intact K1 promoter. Nucleotide positions are given relative to the K1 transcription start site.

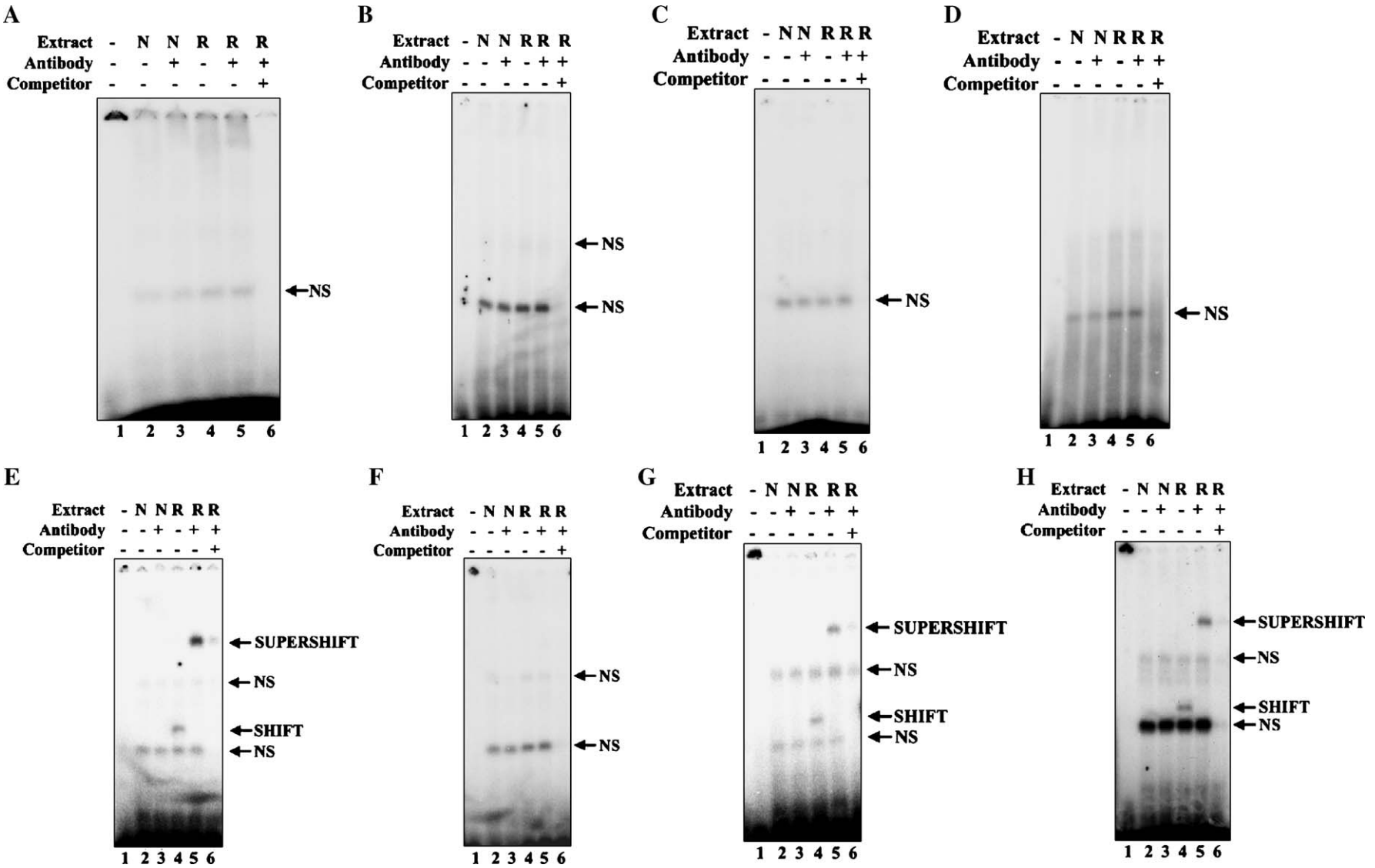

Fig. 5. Identification of Rta-binding sites within the K1 promoter by EMSA analysis. The Rta DNA-binding domain (amino acids 1–320) was expressed in BL21 *E. coli* and purified by Ni-NTA purification. This purified protein was used in EMSA analysis with the panel of K1 promoter probes diagrammed in Fig. 4. Panels A through H represent EMSA analysis with probes A through H shown in Fig. 4, respectively. Rta-specific shifts and supershifts in panels E, G, and H are indicated. Nonspecific (NS) bands are similarly indicated for each EMSA. Lane 1: probe alone, lane 2: untransformed BL21 negative control, lane 3: untransformed BL21 with anti-FLAG antibody, lane 4: Rdbd extract, lane 5: Rdbd extract with anti-FLAG antibody, lane 6: Rdbd extract with anti-FLAG antibody and unlabeled PAN competitor.

binding sites, G and H, correlate with the reduced Rta responsiveness associated with linkers P11 and P18 (Fig. 2A). Mutation of either of these elements reduced but did not completely eliminate Rta responsiveness (Fig. 2A). EMSA probe E corresponds to the region mutated in linker P4, which did not have a significant effect on Rta responsiveness in reporter assays. To completely eliminate the responsiveness to Rta, it may be necessary to mutate two, or perhaps all three Rta-binding sites within the K1 promoter. Double and triple mutations were therefore made to the three K1 Rta-binding sites to analyze their combined contribution to promoter activation. Fig. 6A diagrams these mutant plasmids. As before, these mutations were made in the context of the pGL2-Basic luciferase vector. The single, double or triple K1 promoter mutants were transfected into three different cell lines: KSHV-positive BCBL-1 B cells, KSHV-negative DG75 B cells, and KSHV-negative CV-1 fibroblasts. The promoter mutants were transfected with either a pcDNA3-Rta expression vector or a pcDNA3 plasmid, as well as a β-galactosidase expression plasmid to control for transfection efficiency. As before, mutation of linker P4 had little to no effect on the responsiveness of the K1 promoter to Rta in each cell line tested (Figs. 6B, C, and D). Single mutations of linker P11 and P18 resulted in decreased activation by Rta. In the context of BCBL-1 cells, linker P11 displayed a 5.4-fold activation, while linker P18 was slightly lower with 1.7-fold activation (Fig. 6B).

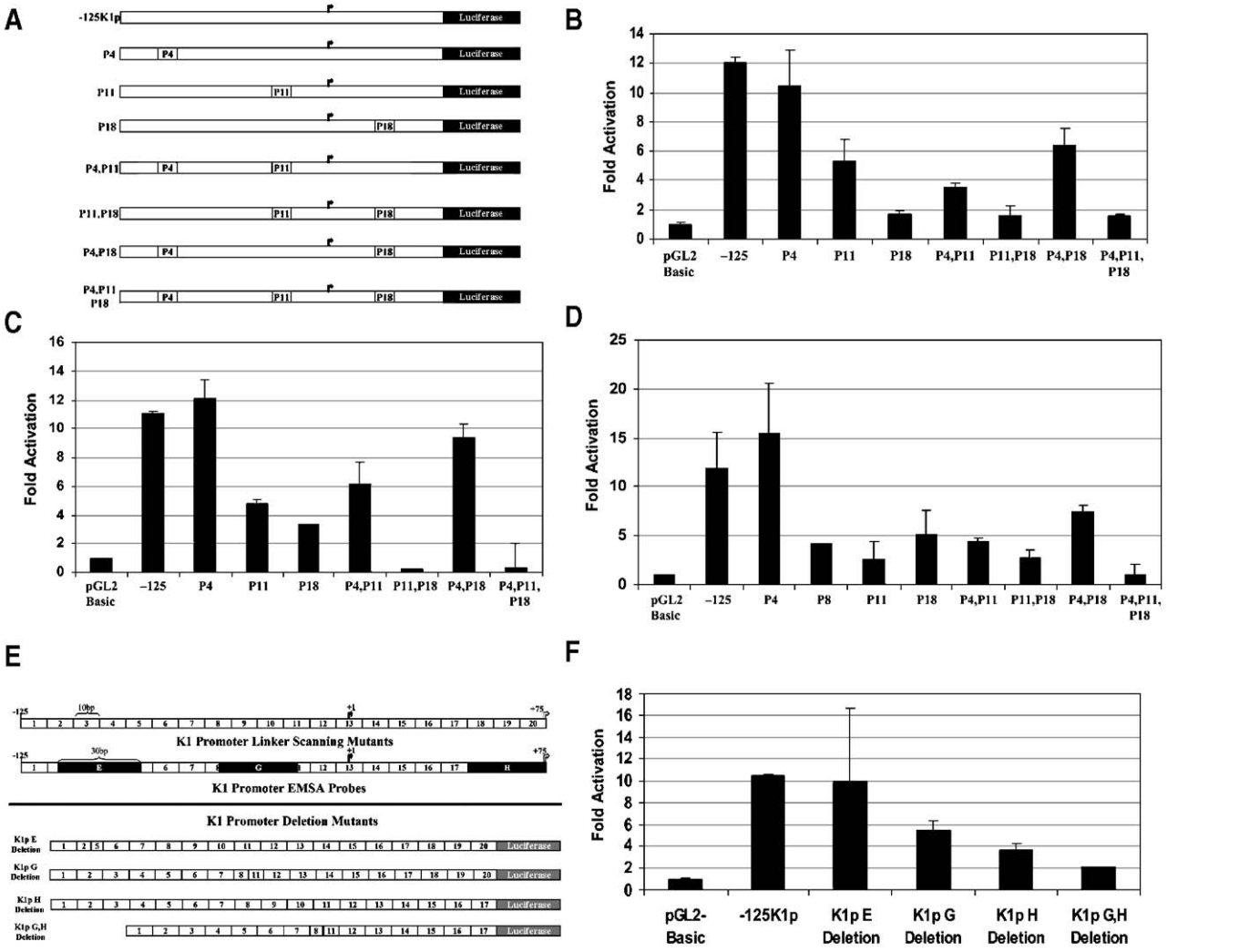

Fig. 6. Analysis of K1 promoter double/triple mutants. (A) Diagram of K1 promoter mutants. In addition to the single linker scanning mutants P4, P11, and P18, a panel of double and triple mutants was generated in the context of the pGL2-Basic luciferase vector. Mutated sequences are indicated by open, labeled boxes. (B, C and D) Double/triple K1 promoter mutant activity in BCBL-1 B cells (B), uninfected DG75 B cells (C), and CV-1 fibroblast cells (D), respectively. Wild-type -125K1p/pGL2-Basic was transfected in parallel with the single, double, and triple mutants as shown in panel A along with a β-galactosidase expression vector to normalize for transfection efficiency and either an Rta expression vector or empty pcDNA3 plasmid as a negative control. The data are represented as fold activation over pcDNA3-transfected controls. (E) Diagram of K1 promoter deletion mutants. A panel of 30-bp deletion mutants was generated that possess 30-bp deletions at each Rta-binding site identified by EMSA analysis. Numbered boxes indicate the location of the 10-bp linker scanning substitutions described previously. Black boxes indicate the three, 30-bp regions identified as Rta-binding sites. (F) Each deletion mutant was transfected into BCBL-1 cells along with a β-galactosidase expression vector to normalize for transfection efficiency and either an Rta expression vector or empty pcDNA3 plasmid as a negative control. The data are represented as fold activation over pcDNA3-transfected controls.

In DG75 B cells, activation of linkers P11 (4.8-fold) and P18 (3.3-fold) was also reduced, but not totally eliminated (Fig. 6C). Finally, in CV-1 cells, linker P11 displayed a 2.6-fold activation by Rta, while linker P18 displayed a 5.2-fold activation by Rta (Fig. 6D).

In each cell line, the P4,P11 and P4,P18 double mutants both had an intermediate response to Rta (Figs. 6B, C, and D). The P11,P18 double mutant and P4,P11,P18 triple mutant, however, both displayed little to no responsiveness to Rta in each cell line (Figs. 6B, C, and D). In summary, these data suggest that linker P4 does not significantly contribute to Rta responsiveness. However, when both P11 and P18 are mutated, the K1 promoter is no longer responsive to Rta, indicating that there are two functionally significant Rta response elements in the K1 promoter.

The EMSA analysis presented in Fig. 5 made use of 30-bp probes, while each K1 promoter luciferase plasmid was designed with one or more 10-bp substitutions (Figs. 2A, 6A). In order to directly compare reporter assay data with EMSA data, a panel of 30-bp K1 promoter deletion mutants was generated for use in luciferase assays. These deletion mutants are diagrammed in Fig. 6E and are designed to separately remove each Rta-binding site identified by EMSA analysis in Fig. 5. In addition, both the G and H Rta-binding sites were removed in the K1p G, H deletion mutant similar to the double substitution mutant P11, P18. These deletion mutants were transfected into BCBL-1 cells with either a pcDNA3-Rta expression vector or pcDNA3 vector, as well as a β-galactosidase expression plasmid to control for transfection efficiency and Rta responsiveness was assessed by luciferase assays. The wild-type −125K1p plasmid was included for comparison.

Deletion of the K1p E Rta-binding site did not affect Rta responsiveness (Fig. 6F), similar to the P4 10-bp substitution mutant used in Figs. 6B, C, and D. Deletion of either the K1p G Rta-binding site or the K1p H Rta-binding site alone reduced the level of Rta responsiveness, while a double deletion mutant that lacks both the K1p G and K1p H Rta-binding sites possessed no Rta responsiveness (Fig. 6F). These data agree with the 10-bp substitution mutant luciferase data and indicate that the G and H Rta-binding sites each contribute to Rta responsiveness. A complete loss of Rta responsiveness occurred only when both the G and H Rta-binding sites were removed. Furthermore, the fold activation for each of the K1 promoter deletion mutants is nearly identical to the fold activation for each 10-bp substitution (Figs. 6B, F). Therefore, these data confirm that the reduced Rta responsiveness observed with the 10-bp substitution mutants P11 and P18 correlates with deletion of the corresponding Rta-binding sites identified by EMSA analysis.

Rta-binding sites G and H impart Rta responsiveness to a heterologous promoter

Each Rta-binding site in the K1 promoter, as identified by EMSA, was cloned upstream of an E4 TATA box in the pE4T/Luc plasmid (Song et al., 2003) to further assess the functional role of these Rta-binding sites. These constructs were named pE4T-$K1_E$, pE4T-$K1_G$, and pE4T-$K1_H$. The full-length, wild-type K1 promoter (−125K1p) was also cloned into the pE4T-Luc vector to demonstrate Rta responsiveness of the full-length K1 promoter in this vector backbone. The pE4T-Luc vector possesses an E4 TATA box cloned upstream of the luciferase gene and has been used previously to study the responsiveness of other Rta response elements to Rta in the context of a heterologous promoter (Song et al., 2003). Each luciferase plasmid was transfected into HEK 293 cells with either a pcDNA3-Rta expression vector or empty pcDNA3 plasmid along with a β-galactosidase expression vector to control for transfection efficiency. The results of this analysis are represented as a fold activation over empty pcDNA3 control vector. In the context of the pE4T-Luc vector, the full-length K1 promoter element was activated approximately 6-fold by the expression of Rta (Fig. 7B). The E-binding site plasmid (pE4T-$K1_E$) was unresponsive to Rta expression. However, the G- and H-binding sites were activated approximately 3-fold by Rta (Fig. 7B). These data indicated that the G and H Rta-binding sites were capable of imparting Rta responsiveness to the heterologous E4 TATA box promoter, and the sum of their activation was equivalent to that of the full-length −125K1p.

Identification of a functional TATA box within the K1 promoter

To confirm that a sequence identified as a putative TATA box in the K1 promoter can function as a TATA box, the putative K1 TATA box was substituted for the SV40 TATA box within the context of the pGL2-Promoter vector as shown in Fig. 7C. The pGL2-Promoter/K1 TATA box plasmid was transfected into DG75 cells, and its activity was determined by luciferase assays as before (Fig. 7D). The activity of the K1 TATA box vector was compared with the promoter-less pGL2-Basic vector and pGL2-Promoter/SV40 TATA. The activity of these plasmids is represented as fold activation over empty pGL2-Basic vector. The pGL2-Promoter/SV40 TATA vector possessed 45.9-fold activity over pGL2-Basic, while pGL2-Promoter/K1 TATA possessed 15.9-fold activity over pGL2-Basic. Although the basal activity of pGL2-Promoter/K1 TATA is less than pGL2-Promoter/SV40 TATA, these data indicate that the sequence identified as a K1 TATA box can be placed in a heterologous promoter context and can effectively function as a TATA box.

TATA box-binding protein (TBP) binds to the K1 TATA box

Electrophoretic mobility shift assays were performed to determine whether the TATA box-binding protein (TBP) could bind to the K1 TATA, TAATTTT. As a positive control for TBP binding, oligonucleotides containing a consensus TATA box (TATAAAA) were included in the EMSA analysis. Incubation of the consensus TATA box probe with purified TBP (Santa Cruz Biotech) resulted in the formation of a complex with reduced mobility (Fig. 8A, lane 2). Incubation with a monoclonal antibody to TBP (Covance, clone ITBP18)

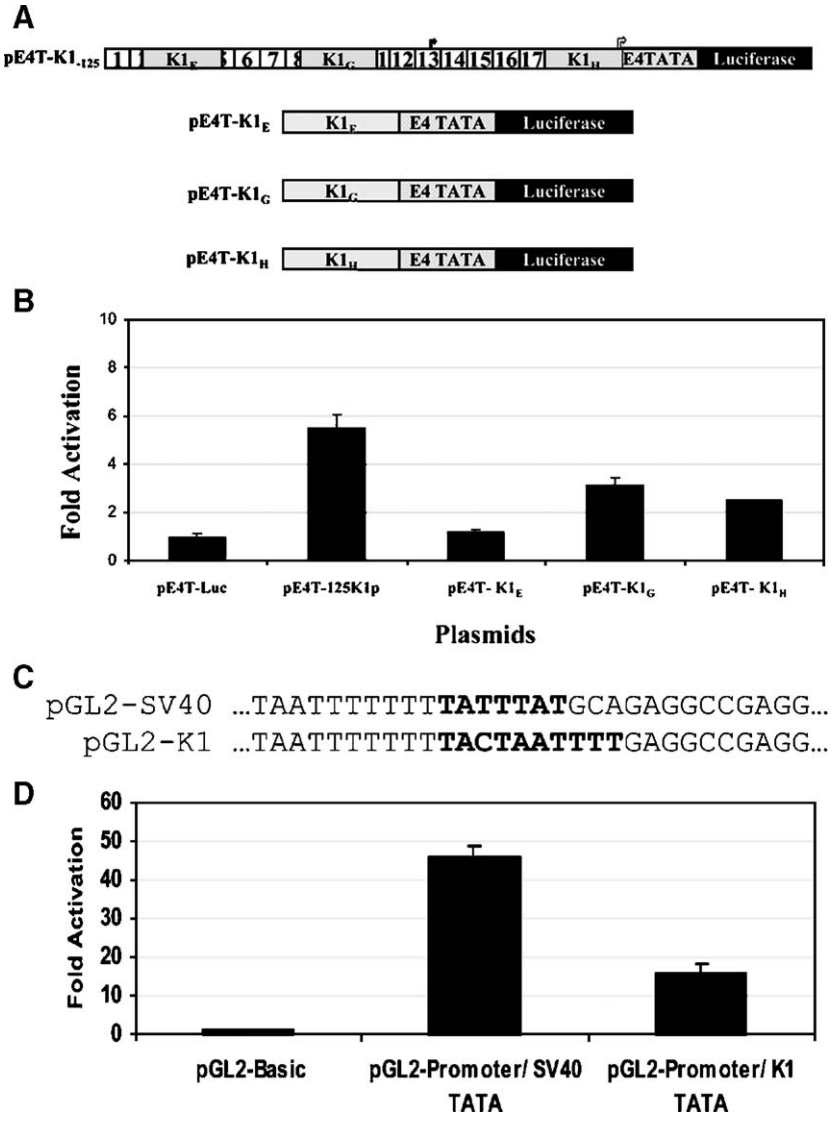

Fig. 7. Rta-binding sites and the K1 TATA box in the context of heterologous promoter elements. (A) Diagram of the E4 TATA box plasmids used to compare K1 Rta responsiveness in the context of a heterologous promoter. The full-length K1 promoter was cloned upstream of the E4 TATA box to indicate K1 promoter activity in the context of the pE4T-Luc vector. $K1_E$, $K1_G$, $K1_H$ were cloned individually upstream of the E4 TATA box. (B) Each E4T luciferase plasmid was transfected into HEK 293 cells along with a β-galactosidase expression vector to normalize for transfection efficiency and either an Rta expression vector or empty pcDNA3 plasmid as a negative control. The data are represented as Rta-fold activation over empty pcDNA3 vector. (C) The K1 TATA box was substituted for the SV40 TATA box in the context of the pGL2-Promoter vector. Bold nucleotides represent the SV40 or K1 TATA box. (D) The pGL2-Promoter/K1 TATA and pGL2-Promoter/SV40 TATA vectors were transfected into DG-75 B cells along with a β-galactosidase expression vector to normalize for transfection efficiency. The data are represented as fold activation over empty pGL2-Basic vector.

resulted in a much weaker shifted band, but no obvious supershifted band (Fig. 8A, lane 3). This may indicate that the binding of the anti-TBP antibody to TBP prevents its association with the probe. Alternatively, this may reflect the formation of a TBP–DNA–antibody complex that is too large to enter the gel. Regardless, these data confirm the presence of TBP in the shifted complex. For further confirmation, an excess of unlabeled consensus TATA box oligonucleotides were incubated with the consensus TATA box probe and TBP and efficiently competed for binding to TBP (Fig. 8A, lane 4).

Similar to the positive control, incubation of the K1 TATA box probe with purified TBP resulted in the appearance of a band with reduced mobility (Fig. 8B, lane 2). Incubation with a monoclonal antibody to TBP (Covance, clone ITBP18) again weakened the shifted band but did not form a supershifted complex (Fig. 8B, lane 3). Finally, incubation of the K1 TATA box probe with TBP and an excess of unlabeled consensus TATA box oligonucleotides inhibited the formation of a shifted band (Fig. 8B, lane 4). These data indicate that TBP binds to the K1 TATA box.

Additional competition experiments were included to confirm the specificity of TBP binding. In Fig. 8C, unlabeled consensus TATA box oligonucleotides (lane 4) or unlabeled K1 TATA box oligonucleotides (lane 5) effectively competed with a consensus TATA box probe for binding to TBP, while

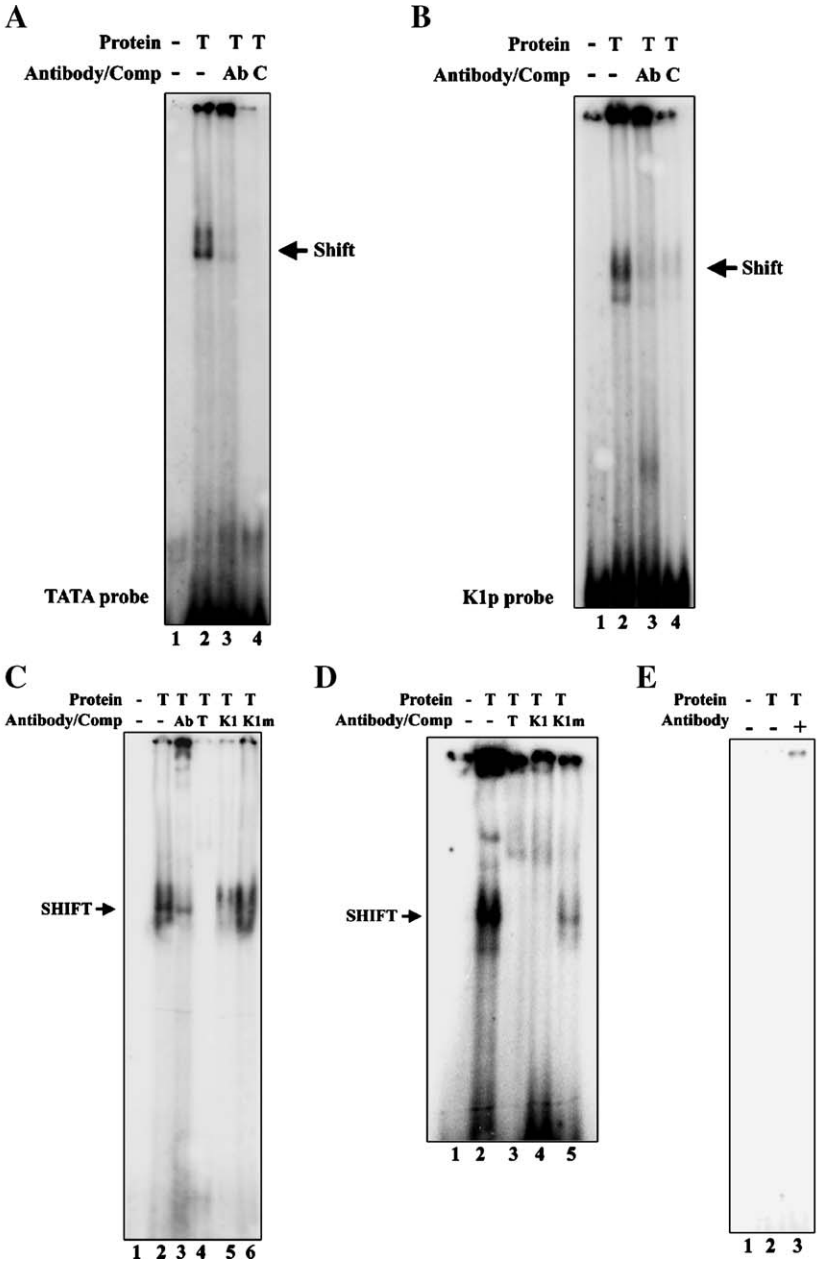

Fig. 8. TBP EMSA analysis of the K1 TATA box. Consensus TATA box oligonucleotides (A, lane 1) and K1 TATA box oligonucleotides (B, lane1) were annealed and ^{32}P-labeled for EMSA analysis. Purified TBP was added to examine complex formation (A, B, lane 2). A monoclonal anti-TBP antibody (Covance) was added (A, B, lane 3) to confirm the presence of TBP in the shifted complex. An excess of unlabeled, annealed consensus TATA box oligonucleotides was added to compete for binding to TBP (A, B, lane 4). Consensus TATA box oligonucleotides (C) or K1 TATA box oligonucleotides (D) were labeled, and the specificity of TBP binding was determined through competition with unlabeled consensus TATA box oligonucleotides (C, lane 4; D, lane 3), K1 TATA box oligonucleotides (C, lane 5; D, lane 4), and mutated K1 TATA box oligonucleotides (C, lane 6; D, lane 5). (E) Mutated K1 TATA box oligonucleotides were labeled and incubated with TBP in the presence (lane 3) or absence (lane 2) of a monoclonal anti-TBP antibody (Covance). Lane 1 depicts probe alone.

unlabeled, mutated K1 TATA box oligonucleotides (lane 6) did not compete for binding to TBP. In Fig. 8D, the reciprocal experiment was performed; unlabeled consensus TATA box oligonucleotides (lane 3) or unlabeled K1 TATA box oligonucleotides (lane 4) competed with a K1 TATA box probe for binding to TBP, while the mutated K1 TATA box oligonucleotides (lane 5) did not compete for binding. Finally, a mutated K1 TATA box probe was unable to bind to TBP (Fig. 8E). These data confirm the specificity of TBP binding.

Coimmunoprecipitation of KSHV Rta with TBP

To determine whether KSHV Rta also interacts with TBP, coimmunoprecipitation experiments were performed. TREx BCBL-Rta cells (Nakamura et al., 2003) were treated with 1 μg of doxycycline/ml for 36 h at 37 °C to induce expression of Rta. Fig. 9A, lanes 1 and 2 represent immunoprecipitations performed with lysates prepared from uninduced TREx-Rta BCBL-1 cells, while lanes 3 and 4 were performed with lysates prepared from doxycycline-induced TREx-Rta BCBL-1 cells.

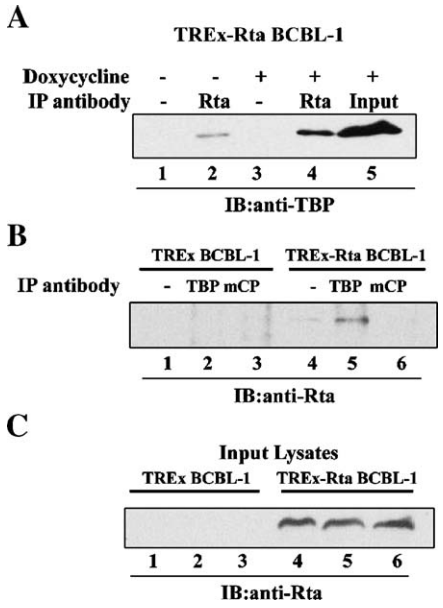

Fig. 9. Coimmunoprecipitation of KSHV Rta with TBP. (A) TREx-Rta BCBL-1 cells were treated with 1 μg doxycycline/ml (lanes 3, 4, 5) or were left untreated for 36 h (lanes 1 and 2). Cell lysates were incubated with a polyclonal anti-Rta antibody to immunoprecipitate Rta (lanes 2 and 4) or no antibody as a negative control (lanes 1 and 3) and were immunoblotted with monoclonal anti-TBP antibody. Input lysate was included to indicate endogenous TBP (lane 5). (B) TREx-RTA BCBL-1 cells (lanes 4, 5, 6) or TREx BCBL-1 cells (lanes 1, 2, 3) were treated with 1 μg doxycycline/ml for 36 h. Cell lysates were incubated with a monoclonal anti-TBP antibody (lanes 2, 5) to immunoprecipitate TBP or anti-HHV8 mCP as an irrelevant antibody control (lanes 3, 6) or no antibody as negative control (lanes 1, 4). Samples were immunoblotted with a polyclonal anti-Rta antibody. (C) TREx-Rta BCBL-1 cells (lanes 4, 5, 6) or TREx BCBL-1 cells (lanes 1, 2, 3) were treated with 1 μg doxycycline/ml for 36 h. Cell lysates were immunoblotted with a polyclonal anti-Rta antibody to demonstrate Rta expression in input lysates.

In the absence of an immunoprecipitating antibody, no TBP was detected (lanes 1 and 3). However, immunoprecipitations performed with a polyclonal anti-RTA antibody efficiently coimmunoprecipitated TBP (lane 4) indicating an interaction of endogenous Rta with TBP. A low level of spontaneous reactivation in these cells also showed that Rta interacted with TBP in uninduced cells (lane 2). Input lysate was included in lane 5 to demonstrate input TBP.

A reciprocal coimmunoprecipitation was performed (Fig. 9, panel B). TREx-RTA BCBL-1 cells or TREx BCBL-1 cells were treated with 1 μg of doxycycline/ml for 36 h at 37 °C then harvested for coimmunoprecipitation analysis. Lanes 1, 2, and 3 represent lysates from the negative control TREx BCBL-1 cell line, while lanes 4, 5, and 6 represent lysates from the inducible TREx-Rta BCBL-1 cell line. Immunoprecipitation with a monoclonal anti-TBP antibody in lane 5 brought down Rta in the inducible cell line, while no Rta was coimmunoprecipitated in the negative control cell line (lane 2). As additional negative controls, lysates were incubated in the absence of anti-TBP (lanes 1 and 4) or in the presence of an irrelevant antibody to HHV8 minor capsid protein (mCP) (lanes 3 and 6). These data demonstrate that KSHV Rta associates with endogenous TBP.

To demonstrate that we had induced Rta expression in the TREx-Rta BCBL-1 cells, Western blots were performed on input cell lysates, and the results of this analysis are shown in Fig. 9, panel C. In lanes 1, 2, and 3, no Rta is induced in the negative control TREx BCBL-1 cell line, as expected. Lanes 4, 5, and 6, however, demonstrate inducible expression of Rta in the TREx-Rta BCBL-1 cell line.

The PAN RRE competes for binding to a K1 RRE

To demonstrate the specificity of Rta for Rta response elements in the K1 promoter, unlabeled, nonspecific oligonucleotides were included in a binding reaction with Rdbd and the PAN probe (Fig. 10A). This nonspecific sequence was unable to compete for binding to Rdbd (lane 4), while unlabeled PAN Rta response element oligonucleotides specifically competed for Rdbd binding (lane 3). These data indicate that Rta binding in these EMSA analyses is not due to nonspecific binding. In addition, we compared the binding affinities of the K1 Rta-binding sites with the PAN RRE (Fig. 10B). The PAN RRE was labeled and used as a probe. Rdbd binding to the PAN RRE was effectively competed with 400 pmol of unlabeled PAN Rta response element oligonucleotides (lane 3). Unlabeled K1 Rta-binding site oligonucleotides were titrated from 400 to 800 pmol to compete with the PAN RRE probe for Rdbd binding (Fig. 10B). Each K1 Rta-binding site effectively competed for

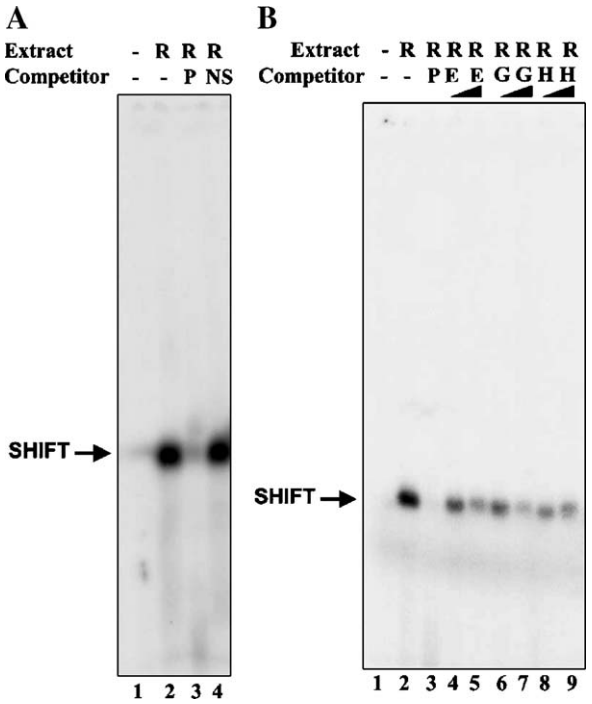

Fig. 10. Confirmation of Rdbd EMSA binding specificity. (A) PAN Rta response element oligonucleotides were labeled and incubated with purified Rdbd in the presence of unlabeled PAN Rta response element oligonucleotides (lane 3) or unlabeled, nonspecific oligonucleotides (lane 4). The arrow indicates an Rta-specific shifted complex. Lane 1: Probe alone, lane 2: Rdbd shift. (B) PAN Rta response element oligonucleotides were labeled and incubated with purified Rdbd in the presence of 400 pmol (lanes 4, 6, and 8) or 800 pmol (lanes 5, 7, and 9) of unlabeled K1 oligonucleotides representing Rta-binding sites E (lanes 4 and 5), G (lanes 6 and 7), and H (lanes 8 and 9). The arrow indicates an Rta-specific shifted complex. Lane 1: Probe alone, lane 2: Rdbd shift, lane 3: Rdbd extract with 400 pmol of unlabeled PAN RRE competitor.

Rdbd, albeit less efficiently than unlabeled PAN RRE oligonucleotides.

Discussion

Several functions have been described for the K1 protein of Kaposi's sarcoma-associated herpesvirus. K1 inhibits apoptosis and initiates signaling pathways that ultimately activate cellular transcription factors (Lagunoff et al., 1999, 2001; Lee et al., 1998a, 1998b; Samaniego et al., 2001; Tomlinson and Damania, 2004). K1 also has been shown to possess transforming properties and to promote the formation of spindle-cell sarcomatoid tumors and malignant plasmablastic lymphomas in K1 transgenic mice (Lee et al., 1998b; Prakash et al., 2002). However, little is known about how K1 transcription is regulated. In our initial characterization of the K1 promoter, we demonstrated that a fully functional promoter element is contained within the first 125 bp upstream of the K1 transcription start site, and that the KSHV immediate-early transcription factor, Rta, activated the K1 promoter above basal levels (Bowser et al., 2002). Here, we explored the mechanism of Rta activation using a panel of linker scanning promoter mutants, reporter assays, coimmunoprecipitations, and electrophoretic mobility shift assays (EMSA).

Linker scanning mutations of promoters have proven to be a useful tool to analyze functional promoter sequences for viral and cellular promoters (Ahn et al., 1992; Hebbar and Archer, 2003; Zeichner et al., 1991). Rta expression activated most of the linker scanning mutants of the K1 promoter to near wild-type levels. However, linkers P8, P9, and P18 demonstrated a greater than 75% reduction in Rta responsiveness in the context of BCBL-1 cells, while linker P11 approached a 75% reduction in responsiveness. Linkers P11 and P18 demonstrated nearly a 75% reduction in Rta responsiveness in the context of DG75 cells. These data suggest that the sequences mutated in linkers P11 and P18 may function as Rta response elements since they showed weakened activity in both cell lines. Interestingly, linkers P8 and P9 demonstrated reduced responsiveness to Rta in the context of BCBL-1 cells but not in the context of DG75 cells. These data raise the possibility that viral-specific factors present in BCBL-1 cells may also contribute to Rta responsiveness.

Reporter analysis of linker P10 only in the context of DG75 B cells resulted in greater activity than the wild-type sequence (Fig. 2B). This increased responsiveness to Rta may reflect the loss of a repressor binding site. Alternatively, these data may reflect the inadvertent introduction of a transcription factor binding site into the K1 promoter element. Although the choice of linker sequence was made to minimize the potential of introducing transcription factor binding sites, when placed in the context of the surrounding K1 promoter sequence, the linker could introduce such sites.

EMSA analysis with a 125-bp fragment of the K1 promoter, which spans much of the functional promoter element, but lacks the 5′ untranslated region indicated that Rta binds directly to the K1 promoter (Fig. 3). EMSA analysis with smaller 30-mer probes that spanned the K1 promoter demonstrated that Rta binds to three sites (E, G, and H) within the K1 promoter element (Figs. 5E, G, and H). Two of these binding sites, E and G, contain sequences similar to the pattern of A/T triplets that have been proposed to function as Rta-binding sites (Liao et al., 2003). Probe E contains the sequence **TTT**CGGGCC**CTTT** which agrees with the $A/T_3N_7A/T_3$ pattern suggested by Liao et al., while probe G contains the sequence **TT**TTCGGCCGG-CCCCTAC**TAATT** which agrees with the $A/T_3N_{17}A/T_3$ pattern (Liao et al., 2003). Interestingly, it has recently been reported that HVS Orf50 contains a DNA-binding domain that has homology to an AT hook DNA-binding motif (Walters et al., 2004). This AT hook motif, present in mammalian high mobility group (HMG)I proteins, has previously been shown to be capable of binding to the minor groove of stretches of AT base pairs (Reeves and Nissen, 1990).

In contrast to probes E and G, probe H does not conform to the A/T triplet pattern and is a unique binding sequence. Rta binding to the vIL-6 core promoter has similarly been shown to occur independent of either A/T triplet pattern (Deng et al., 2002b). Overall, our data demonstrate that two of the three Rta-binding sites identified within the K1 promoter conform to the A/T triplet model for Rta binding. Furthermore, the Rta-binding site identified by probe H represents a unique Rta-binding site that does not conform to the A/T triplet pattern, suggesting the existence of other sequence recognition motifs for this potent viral transactivator.

The identification of three Rta-binding sites suggested that K1 transcriptional activation by Rta could occur via multiple Rta response elements. According to this model, mutation of one Rta response element would reduce, but not totally eliminate Rta responsiveness. This would explain why none of the K1 promoter linker scanning mutants exhibited a total loss of Rta responsiveness. To completely abolish Rta responsiveness, a panel of double and triple mutants was constructed. Reporter assays using these mutants confirmed our hypothesis and identified two functional Rta response elements in the K1 promoter. Rta was unable to activate a double mutant in which the linker P11 and P18 sequences were both mutated (Figs. 6B, C, and D).

Multiple Rta response elements have been discovered within the promoters of other KSHV genes. Rta binds directly to a response element within the PAN promoter located between base pairs −69 and −38, and via an association with RBP-Jk at an RBP-Jk site between base pairs −706 and −1450 (Liang et al., 2002; Song et al., 2001, 2002b). More recently, Wang et al. demonstrated that there are three Rta response elements within the K8 promoter, two of which are regulated differentially based on cell type (Wang et al., 2004). Rta activation of the K8 promoter occurs through both direct binding (Lukac et al., 2001) and through an association with C/EBPα (Wang et al., 2003a). Wang et al. also identified an RBP-Jκ site that may contribute to Rta responsiveness (Wang et al., 2004). However, Rta activation of the K1 promoter involves two functional Rta response elements that both bind directly to Rta. Whether Rta also associates with cellular proteins bound to the K1 promoter remains to be determined. Another characteristic that is unique to the K1 promoter is the presence of an Rta response element within the 5′

untranslated region. Linker P18 corresponds to a mutation in the K1 5′ untranslated region that reduces Rta responsiveness. This is a novel finding since Rta has not been shown to bind to the 5′ untranslated region of other viral genes. However, many cellular transcription factors have been shown to bind to the 5′ UTR of several genes and activate their transcription (Rahaus and Wolff, 1999; van der Stoep et al., 2002).

Each Rta-binding site in the K1 promoter was cloned into the pE4T-Luc vector to determine whether they would be able to impart Rta responsiveness to a heterologous promoter. Interestingly, the $K1_E$ Rta-binding site was unable to impart Rta responsiveness to the E4 TATA vector, while $K1_G$ and $K1_H$ were both able to provide Rta responsiveness (Fig. 7). These data correlate nicely with the information presented in Fig. 6 in that mutation at the $K1_E$ Rta-binding site did not affect Rta responsiveness, but mutation of $K1_G$ and/or $K1_H$ resulted in reduced Rta responsiveness.

In our previous analysis of the K1 promoter, we identified a putative TATA box 25 bp upstream of the K1 transcription start site (Bowser et al., 2002). Here, we demonstrate direct binding of the TATA box binding protein (TBP) to a K1 promoter probe containing the putative TATA box. Interestingly, the K1 TATA box is adjacent to the $K1_G$ Rta-binding site, suggesting the possibility of an interaction between KSHV Rta and TBP on the K1 promoter. We demonstrate here for the first time a direct interaction between the KSHV Rta protein and TBP. Rta may promote transcription of K1 by first binding to the $K1_G$ binding site and then recruiting the polymerase to the K1 TATA box through a direct interaction with TBP. The downstream $K1_H$-binding site may promote transcription through interactions with other factors, such as the TRAP/Mediator coactivator (Gwack et al., 2003).

Materials and methods

Cell culture

KSHV-negative DG75 B cells were grown and maintained in RPMI medium 1640 (Gibco BRL) with L-glutamine and 10% fetal bovine serum (FBS) and supplemented with antibiotics (streptomycin (50 μg/ml) and penicillin (100 U/ml)). KSHV-positive BCBL-1 cells were grown and maintained in RPMI medium 1640 (Gibco BRL) with L-glutamine, 10% fetal bovine serum (FBS), 0.05 mM 2-mercaptoethanol, and 1 mM sodium bicarbonate supplemented with antibiotics (streptomycin (50 μg/ml) and penicillin (100 U/ml)). CV-1 fibroblast cells were grown and maintained in Minimum Essential Medium (Gibco BRL) with Earle's Salts, L-glutamine, and 10% fetal bovine serum (FBS) and supplemented with 0.1 mM nonessential amino acids (Gibco BRL) and antibiotics (streptomycin (50 μg/ml) and penicillin (100 U/ml)). HEK 293 cells were grown and maintained in Dulbecco's modified Eagle's medium (DMEM) (Gibco BRL) with 10% FBS, Glutamax I, high glucose, 110 mg of sodium pyruvate/ml, and pyridoxine–HCl, supplemented with streptomycin (50 μg/ml) and penicillin (100 U/ml). All cell lines were grown and maintained at 37 °C with 5% carbon dioxide.

Plasmids

The luciferase reporter construct −125K1p/pGL2-Basic contains the first 125 bp upstream of the K1 transcription start site and the 5′ untranslated region, cloned into the pGL2-Basic luciferase reporter plasmid (Promega) as previously described (Bowser et al., 2002).

The −125K1p/pGL2-Basic construct was used as a wild-type template for the production of a panel of K1 promoter linker scanning mutants using the Stratagene QuikChange Site-Directed Mutagenesis kit. DNA oligonucleotides were designed to introduce sequential 10-bp substitutions to the wild-type K1 promoter sequence as diagrammed in Fig. 1A. Each primer contained overlapping *Bam*HI and *Nco*I restriction enzyme sites and 15 bp complementary to the wild-type sequence on either side of the target sequence. The primer sequences used to generate this panel of mutants are listed in Table 1. Mutagenesis was performed according to the manufacturer's instructions, with 30 ng of −125K1p/pGL2-Basic as template. Thermocycling conditions were as follows: an initial incubation at 95 °C for 30 s followed by 18 cycles of 95 °C for 30 s, 55 °C for 2 min, and 68 °C for 6 min. Restriction enzyme digests (Fig. 1B) and plasmid DNA sequencing confirmed mutagenesis.

Double and triple mutants of the K1 promoter were generated using the Stratagene QuikChange Site-Directed Mutagenesis kit as before. Linker P4 was used as a template with P11 primers or P18 primers to generate both a P4,P11 and P4,P18 double mutant, respectively. Linker P11 was used as a template in a mutagenesis reaction with P18 primers to generate a P11,P18 double mutant. Finally, the double mutant P4,P11 was used as a template with P18 primers to generate the triple mutant P4,P11,P18. The panel of double and triple promoter mutants is diagrammed in Fig. 6A. Restriction enzyme digests and plasmid sequencing confirmed mutagenesis.

A panel of 30-bp deletion mutants of the K1 promoter was generated using the Stratagene Site-Directed Mutagenesis kit as before. The -125K1p/pGL2-Basic construct was used as a wild-type template for the production of these 30-bp deletion constructs. DNA oligonucleotides were designed to delete each Rta-binding site within the K1 promoter, as diagrammed in Fig. 6E. K1p E deletion 1 5′-AGGCCACGCCTACTTCGAGCGGGGGACGGG-3′; K1p E deletion 2 5′-CCCGTCCCCCGCTCGAAGTAGGCGTGGCCT-3′; K1p G deletion 1 5′-GCTAGGCCACGCCTAAAAGGCGGGGTTCTGC-3′; K1p G deletion 2 5′-GCAGAACCCCGCCTTTTAGGCGTGGCCTAGC-3′; K1p H deletion 1 5′-CCTTGTGTAAACCTGTCTCTCGAGATCTAAGTA-3′; K1p H deletion 2 5′-TACTTAGATCTCGAGAGACAGGTTTACACAAGG-3′. The K1p G deletion mutant was used as a template in a mutagenesis reaction with K1p H oligonucleotides to generate a double deletion mutant that lacks the G and H Rta-binding sites. Restriction enzyme digests and plasmid sequencing confirmed the construction of each plasmid.

Three 30-bp K1 promoter fragments were cloned into the pE4T/Luc vector to determine whether these sequences are sufficient to impart Rta responsiveness. The pE4T/Luc vector contains the E4 TATA box in the context of the pGL3-basic

Table 1
Primers used to make K1 promoter linker scanning mutants

		Primer sequence
Linker P1	Primer A	5′-GGAGGTACCGAGCTCCCATGGATCCTACTTTTTTTTTCGG-3′
	Primer B	3′-CCTCCATGGCTCGAGGGTACCTAGGATGAAAAAAAAAGCC-5′
Linker P2	Primer A	5′-AGCTCAGGCCACGCCCCATGGATCCTTCGGGCCCTTTTTG-3′
	Primer B	3′-TCGAGTCCGGTGCGGGGTACCTAGGAAGCCCGGGAAAAAC-5′
Linker P3	Primer A	5′-ACGCCTACTTTTTTTCCATGGATCCTTTTGGGCGCGCGAG-3′
	Primer B	3′-TGCGGATGAAAAAAAGGTACCTAGGAAAACCCGCGCGCTC-5′
Linker P4	Primer A	5′-TTTTTTTCGGGCCCTCCATGGATCCGCGAGGCGAGCGGGG-3′
	Primer B	3′-AAAAAAAGCCCGGGAGGTACCTAGGCGCTCCGCTCGCCCC-5′
Linker P5	Primer A	5′-GCCCTTTTTGGGCGCCCATGGATCCCGGGGGACGGGGCTA-3′
	Primer B	3′-CGGGAAAAACCCGCGGGTACCTAGGGCCCCCTGCCCCGAT-5′
Linker P6	Primer A	5′-GGCGCGCGAGGCGAGCCATGGATCCGGCTAGGCCACGCCT-3′
	Primer B	3′-CCGCGCGCTCCGCTCGGTACCTAGGCCGATCCGGTGCGGA-5′
Linker P7	Primer A	5′-GCGAGCGGGGGACGGCCATGGATCCCGCCTACTTTTTTTT-3′
	Primer B	3′-CGCTCGCCCCCTGCCGGTACCTAGGGCGGATGAAAAAAAA-3′
Linker P8	Primer A	5′-GACGGGGCTAGGCCACCATGGATCCTTTTTTCGGCCGGCC-3′
	Primer B	3′-CTGCCCCGATCCGGTGGTACCTAGGAAAAAAGCCGGCCGG-5′
Linker P9	Primer A	5′-GGCCACGCCTACTTTCCATGGATCCCGGCCCCTACTAATT-3′
	Primer B	3′-CCGGTGCGGATGAAAGGTACCTAGGGCCGGGGATGATTAA-5′
Linker P10	Primer A	5′-ACTTTTTTTTTCGGCCCATGGATCCTAATTTTCAAAGGCG-3′
	Primer B	3′-TGAAAAAAAAAGCCGGGTACCTAGGATTAAAAGTTTCCGC-5′
Linker P11	Primer A	5′-TCGGCCGGCCCCTACCCATGGATCCAGGCGGGGTTCTGCC-3′
	Primer B	3′-AGCCGGCCGGGGATGGGTACCTAGGTCCGCCCCAAGACGG-5′
Linker P12	Primer A	5′-CCTACTAATTTTCAACCATGGATCCCTGCCAGGCATAGTC-3′
	Primer B	3′-GGATGATTAAAAGTTGGTACCTAGGGACGGTCCGTATCAG-5′
Linker P13	Primer A	5′-TTCAAAGGCGGGGTTCCATGGATCCTAGTCTTTTTTTCTG-3′
	Primer B	3′-AAGTTTCCGCCCCAAGGTACCTAGGATCAGAAAAAAAGAC-5′
Linker P14	Primer A	5′-GGGTTCTGCCAGGCACCATGGATCCTTCTGGCGGCCCTTG-3′
	Primer B	3′-CCCAAGACGGTCCGTGGTACCTAGGAAGACCGCCGGGAAC-5′
Linker P15	Primer A	5′-AGGCATAGTCTTTTTCCATGGATCCCCTTGTGTAAACCTG-3′
	Primer B	3′-TCCGTATCAGAAAAAGGTACCTAGGGGAACACATTTGGAC-5′
Linker P16	Primer A	5′-TTTTTTTCTGGCGGCCCATGGATCCACCTGTCTTTCAGAC-3′
	Primer B	3′-AAAAAAAGACCGCCGGGTACCTAGGTGGACAGAAAGTCTG-5′
Linker P17	Primer A	5′-GCGGCCCTTGTGTAACCATGGATCCCAGACCTTGTTGGAC-3′
	Primer B	3′-CGCCGGGAACACATTGGTACCTAGGGTCTGGAACAACCTG-5′
Linker P18	Primer A	5′-TGTAAACCTGTCTTTCCATGGATCCTGGACATCCTGTACA-3′
	Primer B	3′-ACATTTGGACAGAAAGGTACCTAGGACCTGTAGGACATGT-5′
Linker P19	Primer A	5′-TCTTTCAGACCTTGTCCATGGATCCGTACATCAAGCTCGA-3′
	Primer B	3′-AGAAAGTCTGGAACAGGTACCTAGGCATGTAGTTCGAGCT-5′
Linker P20	Primer A	5′-CTTGTTGGACATCCTCCATGGATCCCTCGAGATCTAAGTA-3′
	Primer B	3′-GAACAACCTGTAGGAGGTACCTAGGGAGCTCTAGATTCAT-5′

Notes. Linkers P1, P2, P19, and P20 contain sequence complementary to the pGL2-Basic vector.

plasmid (Promega), and its construction has been described previously (Song et al., 2003). Oligonucleotides were designed with *Sac*I and *Xho*I restriction enzyme sites to facilitate cloning into the pE4T/Luc multiple cloning site. The following oligonucleotides were used to PCR amplify the K1 promoter Rta-binding sites using −125K1p/pGL2-Basic as template: E4T/K1$_E$ primer 1 5′-CGCCGCGAGCT CTTTTTTTCGGGCCCTTTTTGGGCGCGCGAGG-3′ E4T/K1$_E$ Primer 2 5′-CGCCGCCTCGAGCCTCGCGCGCCCAAAAAGGGCCCGAAAAAAA-3′ E4T/K1$_G$ Primer 1 5′-CGCCGCGAGCTCCTTTTTTTTTTCGGCCGGCCCCTACTAATTTTTC-3′ E4T/K1$_G$ Primer 2 5′-CGCCGCCTCGAGGAAAAATTAGTAGGGGCC GGCCGAAA AAAAAAG-3′ E4T/K1$_H$ Primer 1 5′-CGCCGCGAGCTCTT CAGACCTTGTTGGACA TCCTGTACATCAAG-3′ E4T/K1$_H$ Primer 2 5′-CGCCGCCTCGAGCTTGATGTACA GGATGTCCAACAAGGTCTGAA-3′. PCR was performed using Platinum Pfx DNA polymerase (Invitrogen) according to the manufacturer's directions. Amplified K1 response elements were cut with *Sac*I and *Xho*I restriction enzymes and were inserted into the *Sac*I and *Xho*I sites of the pE4T/Luc vector. The entire K1 promoter element was excised from −125K1p/pGL2-Basic by *Sac*I/*Xho*I double digest and was inserted into the *Sac*I and *Xho*I sites of the pE4T/Luc vector to generate pE4T/K1$_{-125}$. Restriction enzyme digests and plasmid sequencing confirmed the construction of each plasmid.

A K1 TATA box construct was generated in which the SV40 TATA box contained within the pGL2-Promoter vector was replaced with the K1 TATA box sequence, as shown in Fig. 7C. The pGL2-Promoter vector was used as a template in a mutagenesis reaction using the Stratagene Site-Directed Mutagenesis kit, as before. DNA primers were designed as follows: K1 TATA 1-5′-GGCTGACTAATTTTTTTTACTAATTTTGAGGCCGAGGCCGCCTCG-3′, K1 TATA 2-5′-CGAGGCGGCCTCGGCCTCAAAATTAGTAAAAAAAATTAGTCAG CC-3′. Restriction enzyme digests and plasmid

sequencing confirmed the construction of the mutant K1 TATA box plasmid.

A mutant K1 TATA box luciferase plasmid was generated using the Stratagene Site-Directed Mutagenesis kit as before. The −125K1p/pGL2-Basic construct was used as a wild-type template for the production of the K1 TATA mutant plasmid with the following DNA oligonucleotides: K1 TATA mutant 1 5′-TTTTTTTCGGCCGGCCCCTGCGCATTTT CAAA-GGCGGGGTTCTGCC-3′; K1 TATA mutant 2 5′-GGCA-GAACCCCGCCTT TGAAAATGCGCAGGGGCCGGCC-GAAAAAAA-3′. Restriction enzyme digests and plasmid sequencing confirmed the construction of the K1 TATA mutant plasmid.

Transfections

Each luciferase transfection was performed in duplicate or triplicate, and each experiment was repeated five times.

KSHV-negative DG75 B cells and KSHV-positive BCBL-1 B cells were electroporated for luciferase assays. For each transfection, 400 μl of cells in RPMI (no serum, no antibiotics) at a concentration of 5×10^6 to 1×10^7 cells/ml was added to 0.4 cm cuvettes. To measure the promoter activity in the presence of Rta, 15 μg of the appropriate K1 promoter luciferase construct, 15 μg of pcDNA3-Rta (or pcDNA3), and 2 μg of a beta-galactosidase expression plasmid were added to either cell line. The cells were electroporated at 300 V, 950 μF and were added to 4 ml RPMI with 10% FBS and antibiotics. The cells were incubated for 48 h at 37 °C with 5% carbon dioxide. After 48 h, the cells were lysed in 200 μl of Promega reporter lysis buffer for use in luciferase and beta-galactosidase assays.

Transfections of HEK 293 cells and CV-1 African green monkey kidney fibroblast cells were performed using the Superfect transfection reagent (Qiagen). A total of 1.5×10^5 cells were seeded in 6-well plates in Minimal Essential Medium with serum and antibiotics. Cells were grown overnight at 37 °C with 5% CO_2. The cells were transfected with 3 μg of luciferase plasmid, 2 μg of Rta expression vector or pcDNA3 vector, and 1 μg of a β-galactosidase expression vector using 10 μl of Superfect reagent according to the manufacturer's instructions. Following the transfection, the cells were incubated for 48 h at 37 °C with 5% carbon dioxide. The cells were lysed in 200 μl of Promega reporter lysis buffer for use in luciferase and beta-galactosidase assays.

Luciferase assays

Luciferase assays were performed to measure the promoter activity of each luciferase plasmid. Cell lysates were subjected to a single freeze/thaw and were spun at 13,000 rpm for 2 min. The supernatants were collected for luciferase and beta-galactosidase analysis. One hundred microliters of cell lysate was injected with 50 ml of Promega luciferase substrate and luminescence was measured on a LMax luminometer (Molecular Devices). Ten microliters of cell lysate was assayed for beta-galactosidase activity using the Tropix Galacto-Star System (Applied Biosystems) according to the manufacturer's instructions.

In the context of BCBL-1 and DG75 B cells, cotransfection of empty pGL2-Basic vector with an Rta expression vector resulted in higher luciferase activity than pcDNA3-transfected controls, suggesting that Rta activates the empty luciferase vector alone. The activation of empty vector by Rta was subtracted from each luciferase assay to distinguish Rta's activation of the K1 promoter from this background activation, and each sample was normalized to beta-galactosidase activity, as before. Following this adjustment, the values obtained for each Rta-transfected sample were divided by those for the corresponding pcDNA3-transfected control to indicate Rta activation. The duplicates/triplicates for each experiment were averaged, and standard deviations were calculated for each data point.

Rta electrophoretic mobility shift assay (EMSA)

The Rta DNA-binding domain (Rdbd) (amino acids 1-320) has been cloned into the pET22b(+) plasmid for expression in bacteria (Song et al., 2002b). Rta expressed from this vector is FLAG-tagged at its amino terminus and has six histidine residues at its carboxy terminus. The Rdbd plasmid was transformed into BL21(DE3)pLysS *E. coli* (Stratagene), and Rdbd expression was induced with 1 mM IPTG for 2 h at room temperature. Expressed Rdbd was purified via its carboxy terminal histidine residues by Ni-NTA agarose purification as described previously(Song et al., 2002b). Untransformed BL21 cells were also treated with 1 mM IPTG and subjected to Ni-NTA agarose purification for use as a negative control.

The entire 125-bp promoter element was excised from a pGL2-Basic plasmid which contains the 125-bp K1 promoter element but lacks the 5′ untranslated region. The promoter element was excised by *Sac*I/*Xho*I double digest, and the ends were filled-in by Klenow with ^{32}P-dCTP and ^{32}P-dATP. To identify the Rta-binding site(s) within the 125-bp K1 promoter element, a panel of 30-bp K1 promoter oligonucleotides that spans the K1 promoter element was synthesized and is diagrammed in Fig. 4. Probe H corresponds to the first 30 bp upstream of the translation start site. Each probe was designed with 5′ overhangs of 2 guanines to facilitate labeling by Klenow fill-in with ^{32}P-dCTP. A previously identified Rta response element contained within the PAN promoter (PAN2) was also labeled and used to control for Rta binding. The sequence of this oligonucleotide was 5′-GGAAATGGGTGGCT AACCTGTC-CAAAATATG-3′.

EMSA reactions were performed similarly to those described previously (Song et al., 2001). Briefly, labeled probes (5×10^5 cpm) were incubated for 30 min on ice with purified, FLAG-tagged Rdbd protein (or BL21 negative control extract) in binding buffer (10 mM Tris–HCl (pH 7.5), 150 mM KCl, 7.5 mM $MgCl_2$, 1 mM EDTA, 2 μg salmon sperm DNA, 5 μg of BSA, 0.5 mM dithiothreitol, 50 mM β-mercaptoethanol, 5% glycerol). Binding reactions were separated on a 5% acrylamide TGE gel. The gel was dried and exposed to a phosphorimager

screen for 18 h and was scanned on a Molecular Dynamics STORM 840 phosphorimager.

For supershift analysis, purified Rdbd (or BL21 negative control extract) was incubated with labeled K1 promoter probe for 15 min on ice. Following this incubation, 4 μl of monoclonal anti-FLAG antibody (Sigma) was added, and the binding reactions were incubated for an additional 30 min on ice. Competition analysis was also performed to further confirm the specificity of the binding interactions. To compete for Rdbd binding, 400 or 800 pmol of unlabeled PAN2 Rta response element, K1p E Rta-binding sequence, K1p G Rta-binding site, or K1p H Rta-binding site was added to Rdbd, and the binding reactions were incubated on ice for 15 min (Song et al., 2001). Labeled K1 promoter probe was then added, and the mixtures were again incubated for 15 min on ice. Finally, 4 μl of monoclonal anti-FLAG antibody (Sigma) was added, and the binding reactions were incubated on ice for 30 min. The binding reactions were then analyzed as before. To further demonstrate the specificity of Rta binding, 500 ng of poly [dG − dC] · poly [dG − dC] (Sigma) was added to Rdbd prior to the addition of labeled PAN2 Rta response element probe.

TATA binding protein (TBP) EMSA

Consensus TATA box oligonucleotides were designed as follows: TATA 1 5′-gcagagcatataaaatgaggtagga-3′, TATA 2 5′-tcctacctcattttatatgctctgc-3′. K1 TATA box oligonucleotides were designed as follows: K1 TATA 1 5′-ggcggccggcccctactaatttt-caaaggcgggg-3′, K1 TATA 2 5′-ggccccgcctttgaaaattag-taggggccggccg-3′. Mutant K1 TATA box oligonucleotides were designed as follows: K1 TATA mutant 1 5′-ggcggccggccc-ctgcggcggcgcaaaggcgggg-3′, K1 TATA mutant 2 5′-ggccccgcct-ttgcgccgccgc aggggccggccg-3′. The consensus TATA box oligonucleotides, K1 TATA box oligonucleotides, and K1 TATA mutant oligonucleotides were annealed and labeled as before with ^{32}P-dCTP. EMSA-binding reactions were assembled on ice with 10% glycerol, 20 mM Tris (pH 8.0), 10 mM magnesium chloride, 2 mM dithiothreitol (DTT), 80 mM potassium chloride, 1 μg poly (dG:dC)·(dG:dC), and 5 μg of purified TBP (Santa Cruz Biotechnology, Inc). For antibody supershifts, 5 μl of Covance monoclonal anti-TBP antibody (clone ITBP18) was added prior to the addition of probe. For competition experiments, 300 pmol of annealed, unlabeled consensus TATA box oligonucleotides, unlabeled K1 TATA box oligonucleotides, or K1 TATA mutant oligonucleotides was added before the addition of probe. The binding reactions were incubated on ice for 15 min. To each binding reaction, 5×10^5 cpm of labeled probe was added. Binding reactions were incubated on ice for an additional 45 min. The binding reactions were separated on nondenaturing acrylamide gels with 0.5× TBE, 6% acrylamide (19:1 acrylamide:bis), 4 mM magnesium chloride, and 0.02% NP-40. The running buffer contained 0.5× TBE, 4 mM magnesium chloride, and 0.02% NP-40. The gel was dried and exposed to a phosphorimager screen for 18 h and was scanned on a Molecular Dynamics STORM 840 phosphorimager.

Coimmunoprecipitation analysis

TREx-Rta BCBL-1 cells or TREx BCBL-1 cells were grown to approximately 3×10^7 cells per flask and were induced with 1 μg doxycycline/ml or were given an equivalent volume of water as a negative control. The cells were incubated at 37 °C, 5% CO_2 for 36 h, then were harvested in radioimmunoprecipitation lysis buffer for Western blots or NP-40 lysis buffer (150 mM NaCl, 0.1% NP-40, 50 mM Tris–Cl [pH 8.0]) for immunoprecipitations. Coimmunoprecipitation lysates were precleared with protein A/G beads (Santa Cruz Biotechnology; A0704) for 2 h at 4 °C, then incubated with 5 μl of polyclonal anti-RTA antibody, 5 μl of monoclonal anti-TBP (Covance, clone ITBP18) or 5 μl of sheep anti-HHV8 minor capsid protein (mCP) (Exalpha Biologicals, Inc.) for 18 h at 4 °C. Lysates incubated in the absence of antibody were included to serve as negative controls. Protein A/G beads were added and incubated at 4 °C for 4 h. Complexes were washed four times in NP-40 lysis buffer, incubated at 70 °C for 5 min in sodium dodecyl sulfate-polyacrylamide gel electrophoresis (SDS-PAGE) loading buffer and separated on a 10% SDS polyacrylamide gel.

Acknowledgments

We thank Dr. Jae Jung for the TREx-BCBL-1 and TREx-Rta BCBL-1 cell line. We thank Stuart Krall for the assistance with the cell lines. We also thank members of the Damania laboratory for informative discussions and D. Dittmer for manuscript reading. This work was supported by grants from the American Association for Cancer Research (AACR) and NIH grant CA096500 to BD and NIH grant CA91791 to R. Sun. BD is a Leukemia and Lymphoma Society Scholar.

Appendix A. Supplementary data

Supplementary data associated with this article can be found in the online version at doi:10.1016/j.virol.2006.02.007.

References

Ahn, J.K., Pitluk, Z.W., Ward, D.C., 1992. The GC box and TATA transcription control elements in the P38 promoter of the minute virus of mice are necessary and sufficient for transactivation by the nonstructural protein NS1. J. Virol. 66 (6), 3776–3783.

Albrecht, J.C., Nicholas, J., Biller, D., Cameron, K.R., Biesinger, B., Newman, C., Wittmann, S., Craxton, M.A., Coleman, H., Fleckenstein, B., et al., 1992. Primary structure of the herpesvirus saimiri genome. J. Virol. 66 (8), 5047–5058.

Alexander, L., Denenkamp, L., Knapp, A., Auerbach, M., Czajak, S., Damania, B., Desrosiers, R.C., 2000. The Primary Sequence of Rhesus Rhadinovirus Isolate 26-95: sequence similarities to Kaposi's sarcoma herpesvirus and rhesus rhadinovirus isolate 17577. J. Virol. 74 (7), 3388–3398.

Bowser, B.S., DeWire, S.M., Damania, B., 2002. Transcriptional regulation of the K1 gene product of Kaposi's sarcoma-associated herpesvirus. J. Virol. 76 (24), 12574–12583.

Cesarman, E., Chang, Y., Moore, P.S., Said, J.W., Knowles, D.M., 1995. Kaposi's sarcoma-associated herpesvirus-like DNA sequences in AIDS-related body-cavity-based lymphomas. N. Engl. J. Med. 332 (18), 1186–1191.

Chang, P.J., Shedd, D., Gradoville, L., Cho, M.S., Chen, L.W., Chang, J., Miller, G., 2002. Open reading frame 50 protein of Kaposi's sarcoma-associated herpesvirus directly activates the viral PAN and K12 genes by binding to related response elements. J. Virol. 76 (7), 3168–3178.

Chen, J., Ueda, K., Sakakibara, S., Okuno, T., Yamanishi, K., 2000. Transcriptional regulation of the Kaposi's sarcoma-associated herpesvirus viral interferon regulatory factor gene. J. Virol. 74 (18), 8623–8634.

Damania, B., Li, M., Choi, J.K., Alexander, L., Jung, J.U., Desrosiers, R.C., 1999. Identification of the R1 oncogene and its protein product from the Rhadinovirus of Rhesus monkeys. J. Virol. 73 (6), 5123–5131.

Damania, B.J.J., Bowser, B.S., DeWire, S.M., Staudt, M., Dittmer, D.P., 2004. Comparison of the Rta/Orf50 transactivator Proteins of Gamma-2 herpesviruses. J. Virol. 78 (10), 5491–5499.

Deng, H., Chu, J.T., Rettig, M.B., Martinez-Maza, O., Sun, R., 2002a. Rta of the human herpesvirus 8/Kaposi sarcoma-associated herpesvirus up-regulates human interleukin-6 gene expression. Blood 100 (5), 1919–1921.

Deng, H., Song, M.J., Chu, J.T., Sun, R., 2002b. Transcriptional regulation of the interleukin-6 gene of human herpesvirus 8 (Kaposi's sarcoma-associated herpesvirus). J. Virol. 76 (16), 8252–8264.

DeWire, S.M., McVoy, M.A., Damania, B., 2002. Kinetics of expression of rhesus monkey rhadinovirus (RRV) and identification and characterization of a polycistronic transcript encoding the RRV Orf50/Rta, RRV R8, and R8.1 Genes. J. Virol. 76 (19), 9819–9831.

Duan, W., Wang, S., Liu, S., Wood, C., 2001. Characterization of Kaposi's sarcoma-associated herpesvirus/human herpesvirus-8 ORF57 promoter. Arch. Virol. 146 (2), 403–413.

Duboise, S.M., Guo, J., Czajak, S., Desrosiers, R.C., Jung, J.U., 1998. STP and Tip are essential for herpesvirus saimiri oncogenicity. J. Virol. 72 (2), 1308–1313.

Ganem, D., 1998. Human herpesvirus 8 and its role in the genesis of Kaposi's sarcoma. Curr. Clin. Top. Infect. Dis. 18, 237–251.

Goodwin, D.J., Walters, M.S., Smith, P.G., Thurau, M., Fickenscher, H., Whitehouse, A., 2001. Herpesvirus saimiri open reading frame 50 (Rta) protein reactivates the lytic replication cycle in a persistently infected A549 cell line. J. Virol. 75 (8), 4008–4013.

Gradoville, L., Gerlach, J., Grogan, E., Shedd, D., Nikiforow, S., Metroka, C., Miller, G., 2000. Kaposi's sarcoma-associated herpesvirus open reading frame 50/Rta protein activates the entire viral lytic cycle in the HH-B2 primary effusion lymphoma cell line. J. Virol. 74 (13), 6207–6212.

Gwack, Y., Byun, H., Hwang, S., Lim, C., Choe, J., 2001. CREB-binding protein and histone deacetylase regulate the transcriptional activity of Kaposi's sarcoma-associated herpesvirus open reading frame 50. J. Virol. 75 (4), 1909–1917.

Gwack, Y., Baek, H.J., Nakamura, H., Lee, S.H., Meisterernst, M., Roeder, R.G., Jung, J.U., 2003. Principal role of TRAP/Mediator and SWI/SNF complexes in Kaposi's sarcoma-associated herpesvirus RTA-mediated lytic reactivation. Mol. Cell. Biol. 23 (6), 2055–2067.

Haque, M., Chen, J., Ueda, K., Mori, Y., Nakano, K., Hirata, Y., Kanamori, S., Uchiyama, Y., Inagi, R., Okuno, T., Yamanishi, K., 2000. Identification and analysis of the K5 gene of Kaposi's sarcoma-associated herpesvirus. J. Virol. 74 (6), 2867–2875.

Hebbar, P.B., Archer, T.K., 2003. Nuclear factor 1 is required for both hormone-dependent chromatin remodeling and transcriptional activation of the mouse mammary tumor virus promoter. Mol. Cell. Biol. 23 (3), 887–898.

Jeong, J., Papin, J., Dittmer, D., 2001. Differential regulation of the overlapping Kaposi's sarcoma-associated herpesvirus vGCR (orf74) and LANA (orf73) promoters. J. Virol. 75 (4), 1798–1807.

Lagunoff, M., Ganem, D., 1997. The structure and coding organization of the genomic termini of Kaposi's sarcoma-associated herpesvirus. Virology 236 (1), 147–154.

Lagunoff, M., Majeti, R., Weiss, A., Ganem, D., 1999. Deregulated signal transduction by the K1 gene product of Kaposi's sarcoma-associated herpesvirus. Proc. Natl. Acad. Sci. U.S.A. 96 (10), 5704–5709.

Lagunoff, M., Lukac, D.M., Ganem, D., 2001. Immunoreceptor tyrosine-based activation motif-dependent signaling by Kaposi's sarcoma-associated herpesvirus K1 protein: effects on lytic viral replication. J. Virol. 75 (13), 5891–5898.

Lee, H., Guo, J., Li, M., Choi, J.K., DeMaria, M., Rosenzweig, M., Jung, J.U., 1998a. Identification of an immunoreceptor tyrosine-based activation motif of K1 transforming protein of Kaposi's sarcoma-associated herpesvirus. Mol. Cell. Biol. 18 (9), 5219–5228.

Lee, H., Veazey, R., Williams, K., Li, M., Guo, J., Neipel, F., Fleckenstein, B., Lackner, A., Desrosiers, R.C., Jung, J.U., 1998b. Deregulation of cell growth by the K1 gene of Kaposi's sarcoma-associated herpesvirus. Nat. Med. 4 (4), 435–440.

Lee, B.S., Paulose-Murphy, M., Chung, Y.H., Connlole, M., Zeichner, S., Jung, J.U., 2002. Suppression of tetradecanoyl phorbol acetate-induced lytic reactivation of Kaposi's sarcoma-associated herpesvirus by K1 signal transduction. J. Virol. 76 (23), 12185–12199.

Lee, B.S., Connole, M., Tang, Z., Harris, N.L., Jung, J.U., 2003. Structural analysis of the Kaposi's sarcoma-associated herpesvirus K1 protein. J. Virol. 77 (14), 8072–8086.

Liang, Y., Ganem, D., 2004. RBP-J (CSL) is essential for activation of the K14/vGPCR promoter of Kaposi's sarcoma-associated herpesvirus by the lytic switch protein RTA. J. Virol. 78 (13), 6818–6826.

Liang, Y., Chang, J., Lynch, S.J., Lukac, D.M., Ganem, D., 2002. The lytic switch protein of KSHV activates gene expression via functional interaction with RBP-Jkappa (CSL), the target of the Notch signaling pathway. Genes Dev. 16 (15), 1977–1989.

Liao, W., Tang, Y., Kuo, Y.L., Liu, B.Y., Xu, C.J., Giam, C.Z., 2003. Kaposi's sarcoma-associated herpesvirus/human herpesvirus 8 transcriptional activator Rta is an oligomeric DNA-binding protein that interacts with tandem arrays of phased A/T-trinucleotide motifs. J. Virol. 77 (17), 9399–9411.

Liu, S., Pavlova, I.V., Virgin, H.W., Speck, S.H., 2000. Characterization of gammaherpesvirus 68 gene 50 transcription. J. Virol. 74 (4), 2029–2037.

Lukac, D.M., Renne, R., Kirshner, J.R., Ganem, D., 1998. Reactivation of Kaposi's sarcoma-associated herpesvirus infection from latency by expression of the ORF 50 transactivator, a homolog of the EBV R protein. Virology 252 (2), 304–312.

Lukac, D.M., Kirshner, J.R., Ganem, D., 1999. Transcriptional activation by the product of open reading frame 50 of Kaposi's sarcoma-associated herpesvirus is required for lytic viral reactivation in B cells. J. Virol. 73 (11), 9348–9361.

Lukac, D.M., Garibyan, L., Kirshner, J.R., Palmeri, D., Ganem, D., 2001. Dna binding by Kaposi's sarcoma-associated herpesvirus lytic switch protein is necessary for transcriptional activation of two viral delayed early promoters. J. Virol. 75 (15), 6786–6799.

Martin, D.F., Kuppermann, B.D., Wolitz, R.A., Palestine, A.G., Li, H., Robinson, C.A., 1999. Oral ganciclovir for patients with cytomegalovirus retinitis treated with a ganciclovir implant. Roche Ganciclovir Study Group. N. Engl. J. Med. 340 (14), 1063–1070.

Moore, P.S., Chang, Y., 1995. Detection of herpesvirus-like DNA sequences in Kaposi's sarcoma in patients with and without HIV infection. N. Engl. J. Med. 332 (18), 1181–1185.

Murthy, S.C., Trimble, J.J., Desrosiers, R.C., 1989. Deletion mutants of herpesvirus saimiri define an open reading frame necessary for transformation. J. Virol. 63 (8), 3307–3314.

Nakamura, H., Lu, M., Gwack, Y., Souvlis, J., Zeichner, S.L., Jung, J.U., 2003. Global changes in Kaposi's sarcoma-associated virus gene expression patterns following expression of a tetracycline-inducible Rta transactivator. J. Virol. 77 (7), 4205–4220.

Prakash, O., Tang, Z.Y., Peng, X., Coleman, R., Gill, J., Farr, G., Samaniego, F., 2002. Tumorigenesis and aberrant signaling in transgenic mice expressing the human herpesvirus-8 k1 gene. J. Natl. Cancer Inst. 94 (12), 926–935.

Rahaus, M., Wolff, M.H., 1999. Influence of different cellular transcription factors on the regulation of varicella-zoster virus glycoproteins E (gE) and I (gI) UTR's activity. Virus Res. 62 (1), 77–88.

Reeves, R., Nissen, M.S., 1990. The A.T-DNA-binding domain of mammalian high mobility group I chromosomal proteins. A novel peptide motif for recognizing DNA structure. J. Biol. Chem. 265 (15), 8573–8582.

Renne, R., Zhong, W., Herndier, B., McGrath, M., Abbey, N., Kedes, D., Ganem, D., 1996. Lytic growth of Kaposi's sarcoma-associated herpesvirus (human herpesvirus 8) in culture. Nat. Med. 2 (3), 342–346.

Sakakibara, S., Ueda, K., Chen, J., Okuno, T., Yamanishi, K., 2001. Octamer-binding sequence is a key element for the autoregulation of Kaposi's

sarcoma-associated herpesvirus ORF50/Lyta gene expression. J. Virol. 75 (15), 6894–6900.

Samaniego, F., Pati, S., Karp, J., Prakash, O., Bose, D., 2001. Human herpesvirus 8 k1-associated nuclear factor-kappa b-dependent promoter activity: role in Kaposi's sarcoma inflammation? J. Natl. Cancer Inst. Monogr. 28, 15–23.

Song, M.J., Brown, H.J., Wu, T.T., Sun, R., 2001. Transcription activation of polyadenylated nuclear RNA by rta in human herpesvirus 8/Kaposi's sarcoma-associated herpesvirus. J. Virol. 75 (7), 3129–3140.

Song, J., Ohkura, T., Sugimoto, M., Mori, Y., Inagi, R., Yamanishi, K., Yoshizaki, K., Nishimoto, N., 2002a. Human interleukin-6 induces human herpesvirus-8 replication in a body cavity-based lymphoma cell line. J. Med. Virol. 68 (3), 404–411.

Song, M.J., Li, X., Brown, H.J., Sun, R., 2002b. Characterization of interactions between RTA and the promoter of polyadenylated nuclear RNA in Kaposi's sarcoma-associated herpesvirus/human herpesvirus 8. J. Virol. 76 (10), 5000–5013.

Song, M.J., Deng, H., Sun, R., 2003. Comparative study of regulation of RTA-responsive genes in Kaposi's sarcoma-associated herpesvirus/human herpesvirus 8. J. Virol. 77 (17), 9451–9462.

Soulier, J., Grollet, L., Oksenhendler, E., Cacoub, P., Cazals-Hatem, D., Babinet, P., d'Agay, M.F., Clauvel, J.P., Raphael, M., Degos, L., et al., 1995. Kaposi's sarcoma-associated herpesvirus-like DNA sequences in multicentric Castleman's disease. Blood 86 (4), 1276–1280.

Staskus, K.A., Zhong, W., Gebhard, K., Herndier, B., Wang, H., Renne, R., Beneke, J., Pudney, J., Anderson, D.J., Ganem, D., Haase, A.T., 1997. Kaposi's sarcoma-associated herpesvirus gene expression in endothelial (spindle) tumor cells. J. Virol. 71 (1), 715–719.

Staskus, K.A., Sun, R., Miller, G., Racz, P., Jaslowski, A., Metroka, C., Brett-Smith, H., Haase, A.T., 1999. Cellular tropism and viral interleukin-6 expression distinguish human herpesvirus 8 involvement in Kaposi's sarcoma, primary effusion lymphoma, and multicentric Castleman's disease. J. Virol. 73 (5), 4181–4187.

Sun, R., Lin, S.F., Gradoville, L., Yuan, Y., Zhu, F., Miller, G., 1998. A viral gene that activates lytic cycle expression of Kaposi's sarcoma-associated herpesvirus. Proc. Natl. Acad. Sci. U.S.A. 95 (18), 10866–10871.

Tomlinson, C.C., Damania, B., 2004. The K1 protein of Kaposi's sarcoma-associated herpesvirus activates the Akt signaling pathway. J. Virol. 78 (4), 1918–1927.

van der Stoep, N., Quinten, E., van den Elsen, P.J., 2002. Transcriptional regulation of the MHC class II trans-activator (CIITA) promoter III: identification of a novel regulatory region in the 5′-untranslated region and an important role for cAMP-responsive element binding protein 1 and activating transcription factor-1 in CIITA-promoter III transcriptional activation in B lymphocytes. J. Immunol. 169 (9), 5061–5071.

Virgin, H.W.t., Latreille, P., Wamsley, P., Hallsworth, K., Weck, K.E., Dal Canto, A.J., Speck, S.H., 1997. Complete sequence and genomic analysis of murine gammaherpesvirus 68. J. Virol. 71 (8), 5894–5904.

Walters, M.S., Hall, K.T., Whitehouse, A., 2004. The herpesvirus saimiri open reading frame (ORF) 50 (Rta) protein contains an at hook required for binding to the ORF 50 response element in delayed-early promoters. J. Virol. 78 (9), 4936–4942.

Wang, S., Liu, S., Wu, M., Geng, Y., Wood, C., 2001a. Kaposi's sarcoma-associated herpesvirus/human herpesvirus-8 ORF50 gene product contains a potent C-terminal activation domain which activates gene expression via a specific target sequence. Arch. Virol. 146 (7), 1415–1426.

Wang, S., Liu, S., Wu, M.H., Geng, Y., Wood, C., 2001b. Identification of a cellular protein that interacts and synergizes with the RTA (ORF50) protein of Kaposi's sarcoma-associated herpesvirus in transcriptional activation. J. Virol. 75 (24), 11961–11973.

Wang, S.E., Wu, F.Y., Fujimuro, M., Zong, J., Hayward, S.D., Hayward, G.S., 2003a. Role of CCAAT/enhancer-binding protein alpha (C/EBPalpha) in activation of the Kaposi's sarcoma-associated herpesvirus (KSHV) lytic-cycle replication-associated protein (RAP) promoter in cooperation with the KSHV replication and transcription activator (RTA) and RAP. J. Virol. 77 (1), 600–623.

Wang, S.E., Wu, F.Y., Yu, Y., Hayward, G.S., 2003b. CCAAT/enhancer-binding protein-alpha is induced during the early stages of Kaposi's sarcoma-associated herpesvirus (KSHV) lytic cycle reactivation and together with the KSHV replication and transcription activator (RTA) cooperatively stimulates the viral RTA, MTA, and PAN promoters. J. Virol. 77 (17), 9590–9612.

Wang, Y., Chong, O.T., Yuan, Y., 2004. Differential regulation of K8 gene expression in immediate-early and delayed-early stages of Kaposi's sarcoma-associated herpesvirus. Virology 325 (1), 149–163.

West, J.T., Wood, C., 2003. The role of Kaposi's sarcoma-associated herpesvirus/human herpesvirus-8 regulator of transcription activation (RTA) in control of gene expression. Oncogene 22 (33), 5150–5163.

Whitehouse, A., Carr, I.M., Griffiths, J.C., Meredith, D.M., 1997. The herpesvirus saimiri ORF50 gene, encoding a transcriptional activator homologous to the Epstein–Barr virus R protein, is transcribed from two distinct promoters of different temporal phases. J. Virol. 71 (3), 2550–2554.

Wu, T.T., Usherwood, E.J., Stewart, J.P., Nash, A.A., Sun, R., 2000. Rta of murine gammaherpesvirus 68 reactivates the complete lytic cycle from latency. J. Virol. 74 (8), 3659–3667.

Zeichner, S.L., Kim, J.Y., Alwine, J.C., 1991. Linker-scanning mutational analysis of the transcriptional activity of the human immunodeficiency virus type 1 long terminal repeat. J. Virol. 65 (5), 2436–2444.

Zhang, L., Chiu, J., Lin, J.C., 1998. Activation of human herpesvirus 8 (HHV-8) thymidine kinase (TK) TATAA-less promoter by HHV-8 ORF50 gene product is SP1 dependent. DNA Cell Biol. 17 (9), 735–742.

Zhong, W., Wang, H., Herndier, B., Ganem, D., 1996. Restricted expression of Kaposi sarcoma-associated herpesvirus (human herpesvirus 8) genes in Kaposi sarcoma. Proc. Natl. Acad. Sci. U.S.A. 93 (13), 6641–6646.